J Seismol (2017) 21:1251–1275
DOI 10.1007/s10950-017-9665-1

ORIGINAL ARTICLE

Seismic hazard of the Northern Apennines based on 3D seismic sources

L. Martelli · M. Santulin · F. Sani · A. Tamaro · M. Bonini · A. Rebez · G. Corti · D. Slejko

Received: 28 September 2016 / Accepted: 26 April 2017 / Published online: 1 June 2017

Abstract Seismic hazard has been computed for the Northern Apennines in northern Italy based on a new seismogenic zonation. This zonation considers inclined (dipping) planes as seismogenic sources, defined on the basis of all the seismotectonic information available so far. Although these geometries are extremely rough because they simplify with a few inclined elements the totality of faults constituting a source, this model mimics the tectonic style better than that based on horizontal planes. Nevertheless, for a comparison between the new ground motions obtained and those available in the literature, the plane version of the zonation has been developed, where horizontal areas (the standard seismogenic zones), representing the surficial projection of the inclined planes, are used as seismogenic sources.

L. Martelli
Servizio Geologico, Sismico e dei Suoli, Regione Emilia-Romagna, Bologna, Italy

M. Santulin
Istituto Nazionale di Geofisica e Vulcanologia, Sezione di Milano, c/o OGS, Trieste, Italy

F. Sani
Dipartimento di Scienze della Terra, Università degli Studi di Firenze, Florence, Italy

A. Tamaro · A. Rebez · D. Slejko (✉)
Istituto Nazionale di Oceanografia e di Geofisica Sperimentale, Trieste, Italy
e-mail: dslejko@inogs.it
?
M. Bonini · G. Corti
Istituto di Geoscienze e Georisorse, Consiglio Nazionale delle Ricerche, Florence, Italy

Keywords Seismic hazard · Seismogenic sources · Northern Apennines · Italy

1 Introduction

It is good practice in engineering seismology to revise the national seismic hazard map when new science is available or when an earthquake occurs in an unexpected area. A 5- to 10-year time period is generally considered suitable for collecting new data and science to contribute to an updating of a national map. In Italy, the official national seismic hazard map (http://zonesismiche.mi.ingv.it/; OPCM 3519/2006; Stucchi et al. 2011) was developed in 2004, and since the publication of the Italian seismogenic zonation ZS9 (Meletti and Valensise 2004; Meletti et al. 2008), reference documents for the national seismic hazard map, various studies and new data have been published about active tectonics and seismicity (e.g. Boccaletti et al. 2004, 2005, 2011; Basili et al. 2008; Sani et al. 2009; Fantoni and Franciosi 2010; Martelli 2011; Mantovani et al. 2011, 2013; Rogledi 2013; Vannoli et al. 2014; Locati et al. 2016). Specific studies of significant seismic sequences that affected central and northern Italy or of relocation of historical earthquakes have also been published.

Moreover, recent events in the Emilia-Romagna region highlighted unexpectedly large ground motions. The strong motion records of the Italian Accelerometric Network (http://www.protezionecivile.gov.it/jcms/it/ran.wp) of the main shocks of May 20 and 29, 2012 show that in the epicentral areas, the horizontal peak ground acceleration (PGA) reached 0.3 g (http://www.protezionecivile.gov.it/jcms/it/ran.wp). In the same areas, the expected horizontal PGA, obtained considering the rock PGA (0.13 ÷ 0.15 g for a 475-year return period) of the Italian seismic code (http://zonesismiche.mi.ingv.it/; OPCM 3519/ 2006) and the local amplification factor according to studies of local seismic response and seismic microzoning, is between 0.21 and 0.24 g for a return period of 475 years (Martelli et al. 2013; Martelli and Romani 2013b). Also for this reason, some regional seismotectonic studies are in progress for the Northern Apennines, and a preliminary version of a new regional seismogenic zonation has recently been proposed (Martelli et al. 2014).

Considering that the geometry and seismic characterisation of the seismic sources are two of the ingredients that most condition the seismic hazard, the new data and studies highlighted the possibility of a better definition of the potentially seismogenic zones of the Northern Apennines and the central and eastern Po Plain. In the context of an agreement between Istituto Nazionale di Oceanografia e di Geofisica Sperimentale (OGS), Emilia-Romagna Region, National Research Council, University of Firenze and ReLUIS, the updating of the seismic hazard and risk maps of the Northern Apennines at a regional scale has been undertaken.

In the present work, a probabilistic seismic hazard analysis (PSHA), based on new data and a complex characterisation of the seismic sources, has been conducted according to the Cornell (1968) approach, using the formulation of the Crisis 2012 software (Ordaz et al. 2012). In accordance with the existing Italian zonation, the new seismogenic sources were initially considered as horizontal planes (seismogenic zones, SZs), some of which are transversal with respect to the Apenninic trend, and constitute an innovative element of the present zonation. Next, a 3D geometry was defined for the new sources by introducing some complex seismogenic planes, i.e. 3D surfaces with a geometry in agreement with the dominant tectonic style in the SZ. The new hazard estimates show interesting differences with respect to the national ones and point out the influence in the computed ground motions on the surface of a 3D geometry joined with a proper attenuation model.

2 3D seismic sources

A new model of seismogenic sources has been elaborated, taking into account the following available information:

- epicentral distribution of earthquakes from macroseismic and instrumental data, in particular those with M>3 [from the catalogues CPTI15 (Rovida et al. 2016), ISIDe (ISIDe Working Group 2015) and other data from the Istituto Nazionale di Geofisica e Vulcanologia (INGV)];
- maximum observed magnitude (from CPTI15; Rovida et al. 2016);
- focal mechanisms from European-Mediterranean Regional Centriod Moment Tensor (RCMT) catalogue (Pondrelli et al. 2011);
- hypocentral depth of the instrumental events from Italian Seismic Instrumental and parametric Data-basE (ISIDe, ISIDe Working Group 2015);
- geometry, type and kinematics of potentially active or recent (Quaternary) structures, identified on the basis of morphological and structural data and integrated with the information from the database of the Italian seismogenic sources DISS 3.2 (Basili et al. 2008; DISS Working Group 2015) and the available literature.

The collected information has contributed to the definition of a general seismotectonic model for the whole study region and delineation of the geographical boundaries of the seismogenic sources (both in 2D and 3D). Particular attention has been paid to these seismotectonic conditions and seismic history in order to avoid excessive extrapolation of local characteristics that could lead to a "mediation" of the hazard, with underestimation of the hazard of more active structures and overestimation of the less active. In summary, the areas differ mainly because of the geometry and type of observed structures, hypothesised focal mechanisms, depth of hypocentres and number and magnitude of the observed events.

Within each area, the seismotectonic conditions are considered homogeneous. For each zone, a failure mechanism was proposed that is defined by the following:

- geometry of the failure plane (strike and dip);
- fault kinematics (normal, reverse, strike-slip, or mixed);
- average hypocentral depth (range);
- maximum magnitude, which is mostly derived from the maximum recorded magnitude or is estimated from macroseismic historical data.

2.1 Geodynamic framework

The Northern Apennines fold-and-thrust belt has been developing since the late Eocene as a result of the collision between the Adriatic plate and the European margin (Corsica-Sardinia block), after the complete consumption of the intervening Ligurian-Piedmont ocean [western Tethys: Boccaletti et al. (1971)]. The main structure of the Northern Apennines consists of stacked NE-verging tectonic units, the oldest and uppermost of which are the ocean-derived Ligurian Units (Jurassic-Eocene) that overlie the continental, passive, margin-related Tuscan Units (Middle-Late Triassic-Miocene; Fig. 1a, b). The evolution of the Northern Apennines has been framed into different geodynamic models, of which the main ones are the following: (1) slab rollback/slab pull models related to a west-dipping Adriatic lithosphere subduction (e.g. Malinverno and Ryan 1986; Doglioni 1991; Faccenna et al. 2001; Lucente and Speranza 2001; Carminati et al. 2012), (2) models involving slab detachment (Wortel and Spakman 1992; van der Meulen et al. 1999; Di Bucci and Mazzoli 2002), (3) mantle upwelling causing a regional bulge (D'Agostino et al. 2001) and (4) continental lithosphere-scale thrusting (Finetti et al. 2005). Other models propose a transition from east-dipping subduction of Tethyan oceanic crust (Cretaceous-Eocene) to post-Eocene west-dipping lithosphere subduction of the Adriatic plate (Boccaletti et al. 1971; Doglioni et al. 1998; Marroni et al. 2001). In the above-mentioned models, the Tyrrhenian sector is generally viewed as a typical back-arc type basin. The post-collisional (i.e. Miocene-Pliocene) evolution of the Northern Apennines has been generally tied to an extensional regime affecting the internal side of the orogen subsequent to the opening of the Tyrrhenian basin (e.g. Martini and Sagri 1993). Later on, extension followed the forelandward (eastward) migration of the compressive thrust fronts (e.g. Elter et al. 1975). Other interpretations propose a more articulated evolution, in which the hinterland and back-arc area were recompressed, interrupting the extensional regime, between ca. 8.5 and 3.5 Ma (Bonini et al. 2014).

Regarding the main geophysical features, the Northern Apennines are characterised by a marked difference in crustal thickness, the latter being about 20–25 km in the hinterland and up to 35–45 km in the foreland (Cassinis et al. 2005) (Fig. 1b). A high heat flow [>100 mW m^{-2}: Della Vedova et al. (2001)] and positive Bouguer gravity anomaly (Marson et al. 1998) characterise the hinterland sector. Seismicity shows very different characteristics in terms of kinematics and hypocentral depth: shallow seismicity (<20 km) with dominant extensional focal mechanisms affects the hinterland and the divide area of the chain, whereas deeper events (≥20 km) with compressive mechanisms prevail in the foreland. The compressive-deep earthquakes [≥20 up to 60–90 km: Selvaggi and Amato (1992); Chiarabba et al. (2005)] have been variously interpreted depending on the geodynamic model. Generally, these earthquakes are related to ongoing subduction of the Adriatic continental lithosphere beneath the Northern Apennines (Eva and Solarino 1992; Meletti et al. 2000; Amato and Cimini 2001; Piccinini et al. 2006) (Fig. 1b). Other models relate part of this seismicity to the deformation associated with active thrust faults in the Adriatic lithosphere (Collettini et al. 1997; Lavecchia et al. 2003; Finetti et al. 2005).

2.2 Seismic activity and main seismogenic belts

The map of the active and presumably active faults in the Northern Apennines and part of Central Apennines (Fig. 2) has been compiled by integrating the existing literature (e.g. Galadini et al. 2001; Boccaletti et al. 2004) with field surveys conducted in areas where we noted morphostrutural elements of active faulting, where historical and instrumental activity is not related to specific structures, or where the active structures are known but fault kinematics is not constrained satisfactorily.

Based on the pattern of active faulting as well as the distribution of historical and instrumental seismicity, the sector of the Apennines under discussion has been subdivided into five main seismotectonic belts with similar seismic activity, namely (from SW to NE; see Fig. 1a): (1) an internal sector (mostly western and central Tuscany), (2) the belt of north-easternmost intramontane basins (north-eastern and north-western Tuscany, Umbria, western Marche), (3) the axial zone on the Adriatic side (south-western Emilia-Romagna and western Marche), (4) the Pede-Apennine margin and (5) the frontal thrust system buried in the Po Plain, which continues offshore in the Adriatic Sea (Fig. 1a).

These major belts comprise smaller seismogenic zones whose main characteristics are summarised in Table 1 and briefly described in the Appendix. Moreover, the longitudinal continuity of major active structures, mainly normal faults in the internal zones and thrust faults in the external sectors, is interrupted by transverse lineaments along which active faults have been located (Fig. 1). These transverse structures may

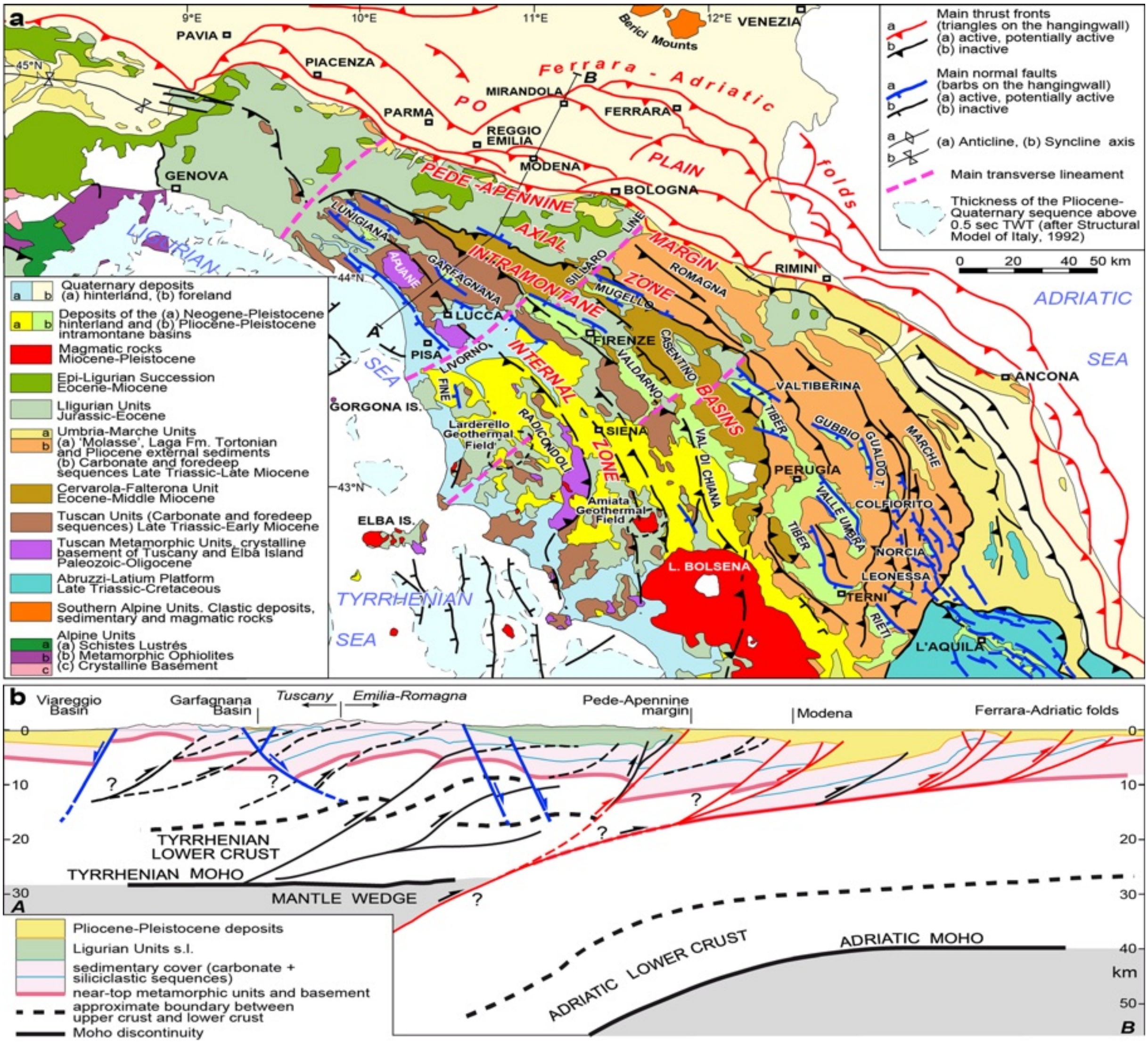

Fig. 1 Geological characteristics of the Northern and Central Apennines: **a** simplified geological map; **b** schematic crustal-lithospheric section AB (see the trace in **a**) through the Apennine wedge (adapted from Bonini 2013)

be seismically important and they have been considered in our new zonation.

The above-reported considerations, as well as the geodynamics of the Northern Apennines, have suggested important modifications to the national zonation ZS9 (Meletti and Valensise 2004; Meletti et al. 2008) and have driven the development of the new zonation proposed here.

2.2.1 Internal belt

The internal belt (Fig. 1a) comprises the Tyrrhenian basin and the numerous marine and continental basins that developed in the hinterland sector (western and central Tuscany) since the Middle-Late Miocene (e.g. Boccaletti and Guazzone 1972). In the classical model, the basins are related to a contiguous extensional regime (e.g. Elter et al. 1975; Brogi and Liotta 2008), whereas in other models, the basins developed under a compressive state that switched to extension during the late stage of basin evolution (e.g. Bonini 1999; Sani et al. 2001). Instrumental seismicity is generally limited and characterised by shallow (<10 km) and low-magnitude (M_W < 4) events (ISIDe Working Group 2015). There are, however, some remarkable exceptions (Fig. 2), particularly the historical seismic events of 1414 ($M_W \approx 5.7$),

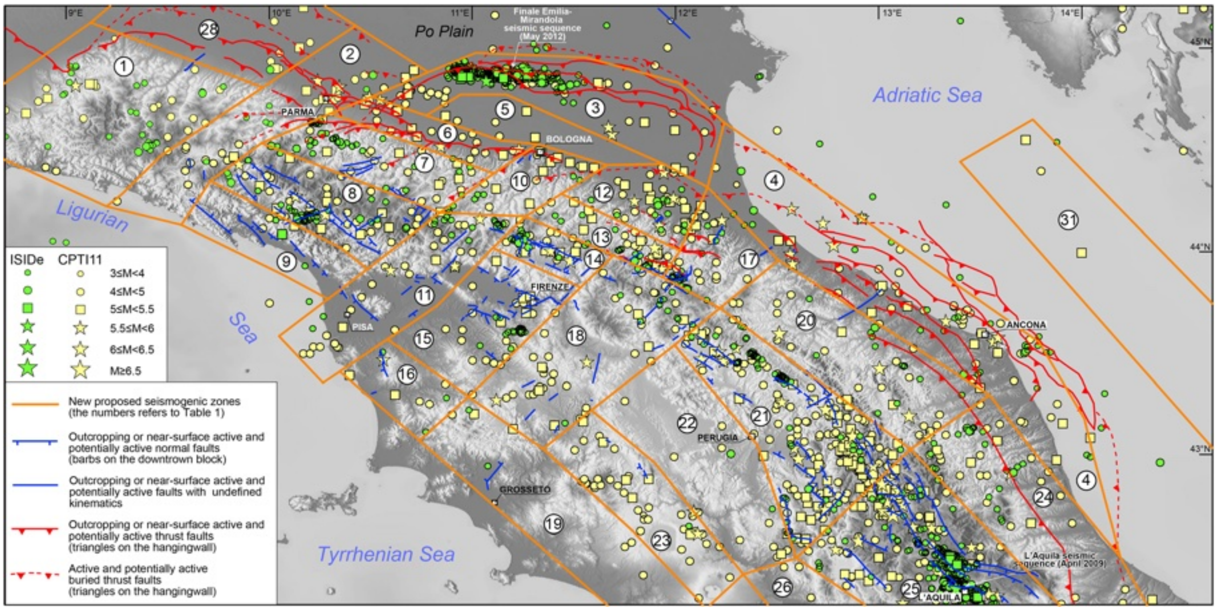

Fig. 2 Active and potentially active faults in the Northern and Central Apennines. Instrumental and historical seismicity is from ISIDe (ISIDe Working Group 2015) and CPTI11 (Rovida et al. 2016) catalogues

1558 ($M_w \approx 6.0$), 1846 ($M_W \approx 6.0$) and 1914 ($M_W \approx 5.6$) that hit the Radicondoli, Val di Fine and Lucca areas, respectively (Rovida et al. 2016). In general, the seismic events cluster in specific areas, particularly the Larderello and Mt. Amiata geothermal fields, Lake Bolsena, around Siena and SW of Florence, the latter seismicity being associated with the recent seismic sequence of December 2014 (Scognamiglio et al. 2009).

The potentially active faults identified are predominantly normal and localised in specific regions, namely the coastal area bordering the Apuane and Monte Pisano massifs, where the faults mostly trend around NW-SE (Figs. 1a and 2). Normal faults with similar orientation have also been identified south of Florence. The presence of transverse (i.e. ca. NE-trending) fault segments is worth mentioning that may be locally important, such as for the Livorno-Sillaro line, SE of Florence and around Siena (Fig. 2). Such transverse faults may be characterised by some component of lateral motion, as inferred from focal mechanism solutions [for instance the moderate earthquakes of September and December 2014 south of Florence and Casentino, respectively (Scognamiglio et al. 2009)].

The following SZs belong to this seismotectonic belt: 9, internal part of 11, 15, 16, internal part of 18, 19, 23 (see Fig. 2).

2.2.2 Belt of intramontane basins (Tyrrhenian side of the main divide)

This zone comprises the belt of continental intramontane basins running on the Tyrrhenian side adjacent to the main topographic divide of the Apennine chain. This belt is relatively narrow in the north-western sector and expands SE-wards. From NW to SE, the main basins are Lunigiana, Garfagnana, Pistoia-Prato-Florence, Mugello, Valdarno, Casentino, Valtiberina, Tiber, Gubbio, Valle Umbra, Colfiorito, Norcia, Leonessa, Rieti and L'Aquila (Fig. 1a). This sector is characterised by widespread seismicity, with seismic events that are generally shallow (<15–20 km depth) and characterised by dominant extensional focal mechanism solutions (Chiarabba et al. 2005, 2015; Pondrelli et al. 2006; Sani et al. 2009; ISIDe Working Group 2015). Importantly, this zone has recorded the strongest seismic events of the Apennines sector considered in this study. In particular, from NW to SE, the strongest historical seismic events ($M_W \geq 6$) are the following (Rovida et al. 2016): Garfagnana 1920 ($M_W \approx 6.5$), Mugello 1919 ($M_W \approx 6.4$), Valtiberina 1352 ($M_W \approx 6.3$), Gualdo Tadino 1751 ($M_W \approx 6.2$), Colfiorito 1279 ($M_W \approx 6.3$), Valle Umbra 1832 ($M_W \approx 6.3$), Norcia 1328 ($M_W \approx 6.5$), Norcia 1703 ($M_W \approx 6.9$), Leonessa 1298 ($M_W \approx 6.3$) and L'Aquila 1703 ($M_W \approx 6.7$). In recent years, this sector has been

Table 1 Main features of the seismogenic sources proposed for the Northern Apennines: orientation of major active fault planes; main or subordinate kinematics of active faults; hypocentral depth range; maximum magnitude

NO.	Dip or trend of main active faults	Kinematics main (subordinate)	Hyp. depth	M_{max}	
				Obs.	*Calc.*
1	NE-SW?	Strike-slip	?	5.7	5.93 ± 0.25
2	NE-SW (S/45–60)	Strike-slip (thrust)	5–30	5.5	5.71 ± 0.29
3	S-SSW/45	Thrust	5–15	6.1	5.94 ± 0.24
4	SW/30	Thrust	5–15	6.1	6.16 ± 0.21
5	S-SSW/15–30	Thrust	15–35	5.5	6.00 ± 0.53
6	S/45–60	Thrust	10–30	6	6.31 ± 0.29
7	N/65 (S/30)	Normal (thrust)	5–10 (>15)	5.5	5.61 ± 0.23
8	NE/60–70(60%) SW/60–70(40%) (NE-SW)	Normal (transtens. Dx)	5–15 (10–20)	6.5 (5.1)	6.50 ± 0.23
9	SW/65 (NE65)	Normal	5–15	5.4	6.28 ± 0.27
10	NNE-SSW (S/45–60)	Strike-slip (thrust)	5–15 (15–35)	5.5	5.73 ± 0.30
11	NE-SW (SW/60–70)	Strike-slip (normal)	5–15	5.7	6.12 ± 0.38
12	S/30–45	Thrust	5–35	6.1	6.23 ± 0.24
13	NE/65 (SSW 30)	Normal (thrust)	3–10 (>15)	6	6.18 ± 0.22
14	SSW/60–70(60%) NNE/60–70(40%)	Normal	5–15	6.3	6.61 ± 0.29
15	SW/65 (NE-SW)	Normal (strike-slip)	5–15	5.4	5.81 ± 0.37
16	WSW/ 60–70	Normal	5–15	5.9	6.43 ± 0.38
17	NNE-SSW (SSW/30)	Strike-slip (thrust)	5–15 (15–25)	6	5.96 ± 0.26
18	NE-SW (SW/60–70?)	Strike-slip (normal?)	5–15	5.8	6.00 ± 0.29
19	SW/ 60	Normal	5–15?	5.1	5.32 ± 0.20
20	SW/30	Thrust	10–35	6.4	6.61 ± 0.29
21	SW/45–65(60%) ENE/45–65(40%)	Normal	5–15	6.7 (6.43)	6.46 ± 0.21
22	WSW/65	Normal	5–15	5.0	5.83 ± 0.40
23	WSW/65	Normal	5–15	5.7	5.97 ± 0.26
24	SW/30	Thrust	10–35	5.5 (6.84)	7.20 ± 0.28
25	SW/50–70	Normal	5–15	7.1	7.06 ± 0.21
26	SW/60–70	Normal	5–15	5.5	5.65 ± 0.25
27	NW/60	Normal	5–15	5.5	5.65 ± 0.25
28	S/45	Thrust	5–30	5.5	5.86 ± 0.46
29	N/30	Thrust	5–15	6.0	6.03 ± 0.30
30	N/30	Thrust	5–15	6.0	5.93 ± 0.24
31	E/35	Thrust	5–15	6.0 (5.43)	5.61 ± 0.23

obs. maximum observed, *calc.* maximum calculated (Kijko and Graham 1998)

affected by destructive earthquakes that caused severe damage in a wide area around the epicentres, particularly the seismic sequences that hit Colfiorito ($M_W \approx 6.0$) on September 1997 and L'Aquila ($M_W \approx 6.3$) on April 2009. The main seismic events are intimately associated with the NW-SE-trending normal fault systems (Fig. 2) that typically border the intramontane basins (Collettini et al. 2005; Chiarabba et al. 2009; Sani et al. 2009; DISS Working Group 2015).

The SZs that belong to this seismotectonic belt are as follows: 8, 14, 21, 22, part of 25 and part of transverse SZs 11 and 18 (see Fig. 2).

2.2.3 The axial zone (Adriatic side)

The axial zone, on the Adriatic side, is still characterised by a widespread seismicity; yet, it is deeper with respect to the belt of intramontane basins. More specifically, focal depths often fall in the range of 20–60 km, particularly in the north-western region [Parma-Modena Apennines: ISIDe Working Group (2015)]. Strong historical events ($M_W \geq 6$) are fewer than in the belt of intermontane basins and reach lower magnitude (computed on macroseismic data). The biggest historical seismic events ($M_W \geq 6$) from NW to SE are the following (Rovida et al. 2016): Romagna Apennines 1661 ($M_W \approx 6.1$), Cagli 1781 ($M_W \approx 6.5$), Fabriano 1741 ($M_W \approx 6.2$), Marche Apennines 1799 ($M_W \approx 6.2$) and 1873 ($M_W \approx 5.9$). The occurrence in the Romagna Apennines of strong earthquakes with $M_W \approx 6.0$ in 1584, 1768 and 1918 is worth mentioning. The focal mechanism solutions are predominantly extensional for shallow events and compressional for earthquakes deeper than 20 km. In the north-western part of the axial zone (Parma-Modena Apennines), surface deformation is characterised by Quaternary normal faults dipping mostly to the north-NE and superimposed onto previous compressive structures (Bonini 2013) (Fig. 2). Similar structures and relationships have been identified in the Romagna Apennines (Fig. 1a, b). In the DISS 3.2 database (DISS Working Group 2015), a gently (SW-)dipping, deep thrust is proposed to be the seismogenic source for the strong historical earthquakes that hit the western Marche. This structure, which is expected to surface along the Marche coastal area, is traced further NW-wards beneath the Romagna and Emilia Apennines. In this scenario, the normal faults and the extensional focal mechanism solutions would represent a shallower response to the deeper thrust activity, in a similar fashion to that inferred for the Bologna Apennines (Picotti and Pazzaglia 2008).

The following SZs are included in this seismotectonic belt: 1, part of transverse zone 2, 7, part of 10, 13, 17, 20 and part of 25 (see Fig. 2).

2.2.4 Pede-Apennine margin

The Pede-Apennine margin represents the sector connecting the exposed Apennine wedge to the Po Plain (Fig. 1). Instrumental seismicity is important but not densely distributed, as it clusters in sectors that have experienced recent seismic sequences [i.e. the 2000 Faenza sequence: ISIDe Working Group (2015)]. Strong historical seismic events are rare and barely reach a macroseismic magnitude of $M_W = 6$. The most important earthquakes (Rovida et al. 2016) are those of Sassuolo 1501 ($M_W \approx 6.1$) and Faenza 1781 ($M_W \approx 6.1$). The available focal mechanism solutions are predominantly compressive with ~N-to-NE-trending P axes, and with hypocentres generally deeper than 15–20 km (e.g. Boccaletti et al. 2004). The Pede-Apennine margin corresponds to a roughly continuous system of SW-dipping thrusts (Pieri and Groppi 1981; Boccaletti et al. 1985; Castellarin et al. 1985) that are responsible for the rapid uplift of the Apennine belt (Doglioni et al. 1999) (Fig. 1). This thrust system can be traced for more than 300 km (Boccaletti et al. 2004, 2011) and is characterised by active thrust segments that may surface in specific sectors (Benedetti et al. 2003; Boccaletti et al. 2011; Bonini 2013; DISS Working Group 2015). The Po Plain closes SE-wards, and seemingly, the Pede-Apennine thrust system continues with the coastal thrust folds of Marche (Vannoli et al. 2014) (Figs. 1 and 2). The latter are characterised by significant seismic events, the most important ($M_W \approx 5.8$) being the Senigallia earthquake of 1930 (Rovida et al. 2016).

The following SZs belong to this seismotectonic belt: part of 28, part of 2, 6, external part of 10, 12 and external part of 17 (see Fig. 2).

2.2.5 The frontal thrust system buried in the Po Plain

An important system of SSW-SW-dipping blind thrusts and folds, typically exhibiting a general arcuate trace in map view, is buried beneath the Po Plain deposits, before the Pede-Apennine margin (Pieri and Groppi 1981; Barberi and Scandone 1983). These structures controlled the deposition of very thick successions of Messinian-Early Pleistocene marine sediments that filled piggyback basins now buried beneath the Middle Pleistocene-Holocene continental deposits of the Po Plain (Pieri and Groppi 1981; Rossi et al. 2002). This underground belt forms the leading edge of the Northern Apennines wedge, which is represented by the external arc connecting Reggio Emilia and Ferrara (Fig. 1a). This external arc can be traced to extend SE-wards offshore of Romagna and Marche [Ferrara-Adriatic folds in Pieri and Groppi (1981)], where it gets closer to the southward continuation of the Pede-Apennine thrust system (Figs. 1a and 2). The recent and ongoing activity of the external Ferrara-Adriatic folds is manifested by the deformation of Middle-Late Pleistocene deposits (Boccaletti et al. 2004, 2011), as well as by the seismic activity that remarkably follows its plan-view shape. The seismicity is generally shallow (≤10 km) and the epicentres mostly cluster in sectors (along the Ferrara-

Adriatic folds) that have been struck by recent seismic sequences, particularly those of Reggio Emilia (October 1996) and Finale Emilia-Mirandola (May 2012) (ISIDe Working Group 2015) (Fig. 2). The historical seismic events in the Po Plain have macroseismic magnitude lower than $M_W \approx 5.6$ (Rovida et al. 2016), and thus, the main shock of the 2012 seismic sequence [which is estimated at $M_W = 6.1$; Pondrelli et al. (2012)] is the largest seismic event recorded so far in this region. Other relevant historical seismic events seemingly related to the Ferrara-Adriatic arc occurred offshore of Rimini in 1916 [$M_W = 5.8$: Rovida et al. (2016)] (Fig. 2). The available fault-plane solutions in the WNW-ESE-trending sector of the arc show a dominant compressive kinematics with N-to-NE-trending subhorizontal P axes, such as for the aforementioned 2012 Emilia seismic sequence (Pondrelli et al. 2012). In the NE-trending lateral thrust ramp, NE of Reggio Emilia, the focal solutions indicate a consistent left-lateral transpression (Ciaccio and Chiarabba 2002).

Within this sector, the following SZs have been individuated: 3, 4, 5, part of 28 and the easternmost part of 2 (see Fig. 2).

3 Seismic hazard

An earthquake catalogue suitable for the seismic hazard assessment of the Northern Apennines has been assembled using the data contained in the catalogues CPTI11 (Rovida et al. 2011), CSI (Castello et al. 2006) and ISIDe (ISIDe Working Group 2015). All duplicated events have been removed using a program to detect them and giving priority to the historical data from CPTI11. The duplicated events have been evaluated case by case using expert judgement, and the dependent events have been eliminated by using the standard space and time declustering algorithm of Gardner and Knopoff (1974) with the same parameters as in California. The obtained catalogue contains 5617 main shocks with magnitude M_W larger than, or equal to, 3.0, in the time window 1000 to 2013. When not available, M_W has been computed by the Gasperini (2004) scaling law.

No background zones have been introduced, because the considered seismic sources cover the whole territory and an additional SZ collects the offshore earthquakes (see the SZ Central Adriatic in Fig. 3).

The seismicity in each seismic source has been modelled according to the untruncated Gutenberg-Richter (GR) distribution (see the GR graphs in Fig. 4), with a threshold magnitude variable from one source to another. More precisely, the maximum likelihood method (MLM) according to the formulation proposed by Weichert (1980) has been applied for the a- and b-values of the G-R relation computation, with the least square method (LSM) considered as well (because, although not formally correct, it sometimes fits the high-magnitude data better), but only as a control of the MLM estimates. It can be seen (Fig. 4) that the MLM fit is good for all SZs and close to the LSM fit. Only in a few cases (SZs 5, 16, 17 and 20) do the seismicity rates seem not to follow a linear trend.

The maximum magnitude M_{max} for each seismic source has been calculated by the Kijko and Graham (1998) statistical algorithm. This procedure can be applied when a frequency-magnitude distribution for the seismic sources is assumed, but also in the extreme case when no information about the nature of the earthquake magnitude distribution is available. The Kijko and Graham (1998) approach computes M_{max} for a source on a statistical basis using the following as input data: the maximum observed magnitude, the threshold magnitude considered complete in the catalogue, the average error in the magnitude estimates (arbitrarily fixed in our case at 0.2), the b-value of the G-R relation and its standard deviation, the annual rate (i.e. the number of earthquakes with magnitude greater than, or equal to, the threshold magnitude) and the catalogue time span which is considered complete (variable according to the minimum magnitude considered).

Since the seminal work of Cauzzi and Faccioli (2008), the same authors with some co-authors have developed a suite of ground motion prediction equations (GMPEs) based on well-controlled global strong motion data (see in Fig. 5 a comparison of the various relations). It can be seen that in the GMPEs of Faccioli et al. (2010) and Cauzzi et al. (2014), a magnitude-dependent distance saturation term models the attenuation in the near field. The last version of this attenuation model (Cauzzi et al. 2014, CAU hereafter) has been selected for modelling the attenuation, because it is considered robust and it is defined for application in different tectonic environments. Moreover, it provides a formulation for rupture distance, which, together with the hypocentral distance, seems suitable for a correct computation of the attenuation, especially in the case of sources with variable depths (inclined planes).

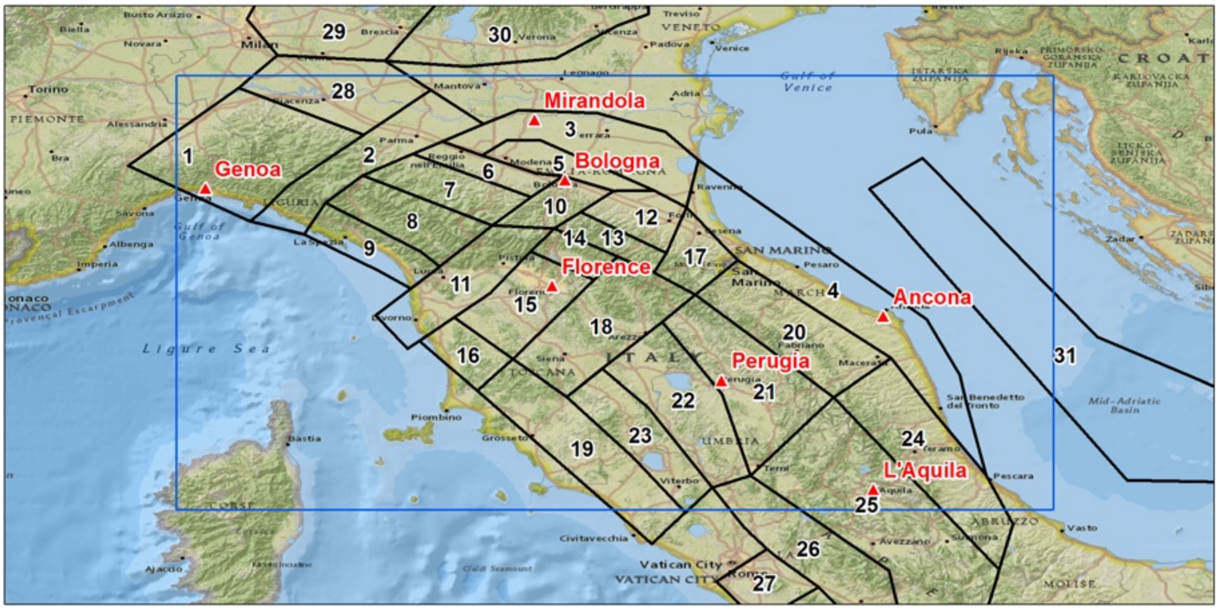

Fig. 3 2D seismogenic model of the Northern Apennines

The computer program Crisis 2012 (Ordaz et al. 2012) has been employed for the computation of the expected ground motion in terms of maps and uniform hazard response spectra for the main settlements in the study region. As a return period (RP), we have considered the standard reference for normal building design according to the European (CEN 2002) and Italian (NTC 2008) building codes, i.e. 475 years, corresponding to a 10% exceedance probability in 50 years. In addition, we have also considered three RPs for strategic buildings: 101, 950 and 1950 years, corresponding to three requirements of the Italian building code (NTC 2008), respectively, for damage, for human survival and for collapse.

3.1 Seismic hazard with 2D sources

The first application of the new seismogenic zonation considered in the present study (Fig. 3) models sources in the usual way, i.e. as superficial plains (SZs), in accordance with the Italian seismic hazard map MPS04 (Stucchi et al. 2011). After a first elaboration with undiversified GMPEs according to the tectonic style of the seismogenic source (Santulin et al. 2014), the specific tectonic style of the different SZs has been taken into account (see Table 1) and the proper CAU GMPE has been applied. Figure 6 shows the expected ground motion, in terms of horizontal PGA obtained for the four considered RPs. For a 101-year RP, it can be seen (Fig. 6a) that the largest hazard is concentrated in the northern end of the Apennines. More precisely, a PGA between 0.15 and 0.175 g has been estimated for the SZ Romagna Apennines (No. 13 in Fig. 3 and Table 1), and a PGA larger than 0.125 g refers to the SZs Emilia Apennines and Garfagnana (Nos. 7 and 8 in Fig. 3 and Table 1). A PGA between 0.125 and 0.150 g can also be seen in a wide area of the Central Apennines (SZs Umbria and Abruzzo, Nos. 21 and 25 in Fig. 3 and Table 1). Similar features are also shown for the other maps with an expected increase in shaking with the increasing RP (particularly evident for the SZ Abruzzo, No. 25 in Fig. 3 and Table 1). It is quite interesting to pinpoint the size of the area with the largest expected PGA, which increases to also cover SZ Mugello (No. 14 in Fig. 3 and Table 1) when an RP of 475 years or more is considered. An additional area with strong expected ground motion (larger 0.30 g for a 1950-year RP, see Fig. 6d) can be found all along the Adriatic coastline (SZs 3 Ferrara and Adriatic Folds, Nos. 3 and 4 in Fig. 3 and Table 1).

3.2 Seismic hazard with 3D sources

Seismic sources representing the real fault geometry associated with related seismicity constitute the target model for describing the seismogenesis of a region. Such a model is not (or only in specific regions) applicable,

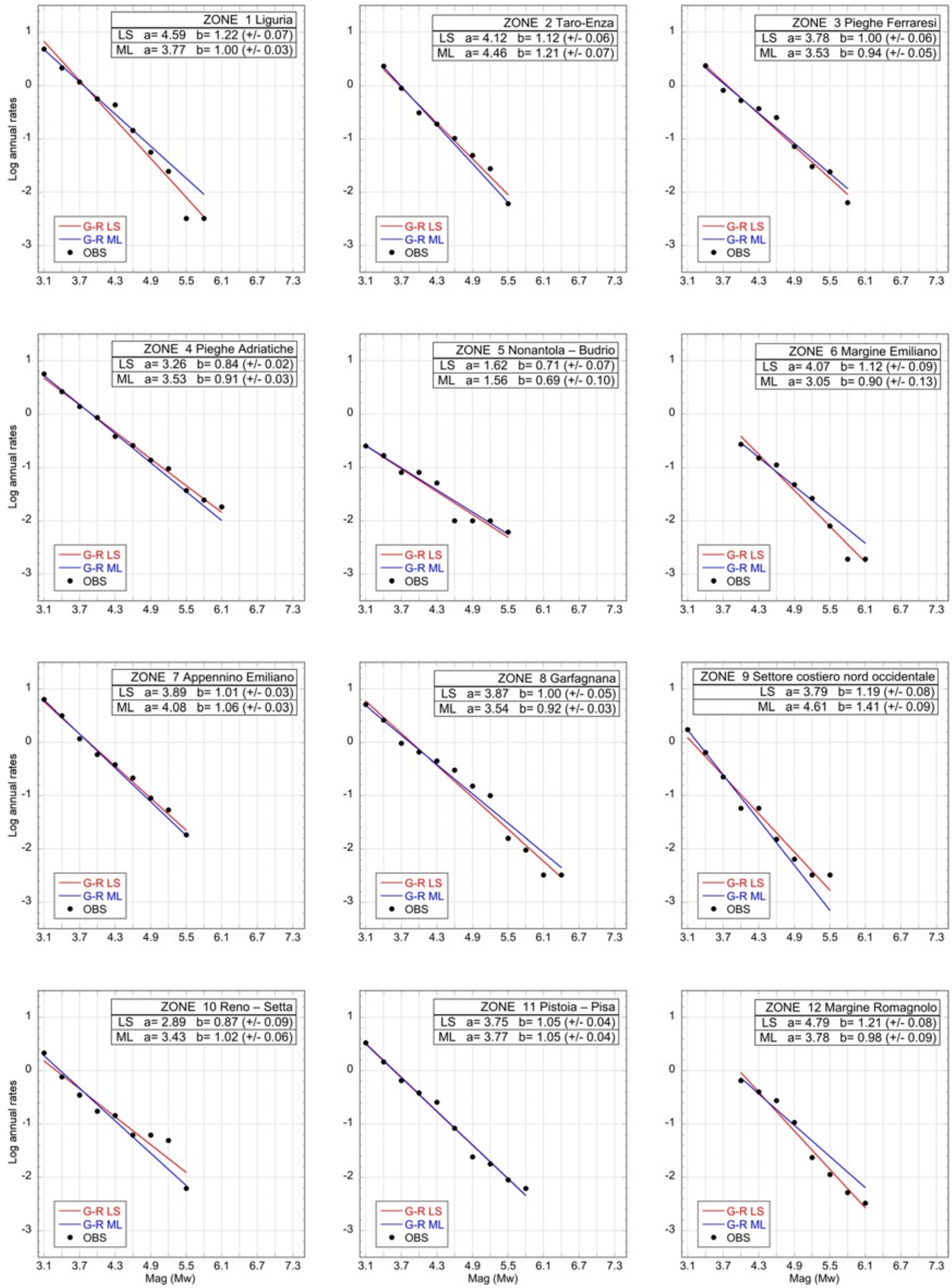

Fig. 4 GR graphs for the SZs: *black line* = MLM, *red line* = LSM

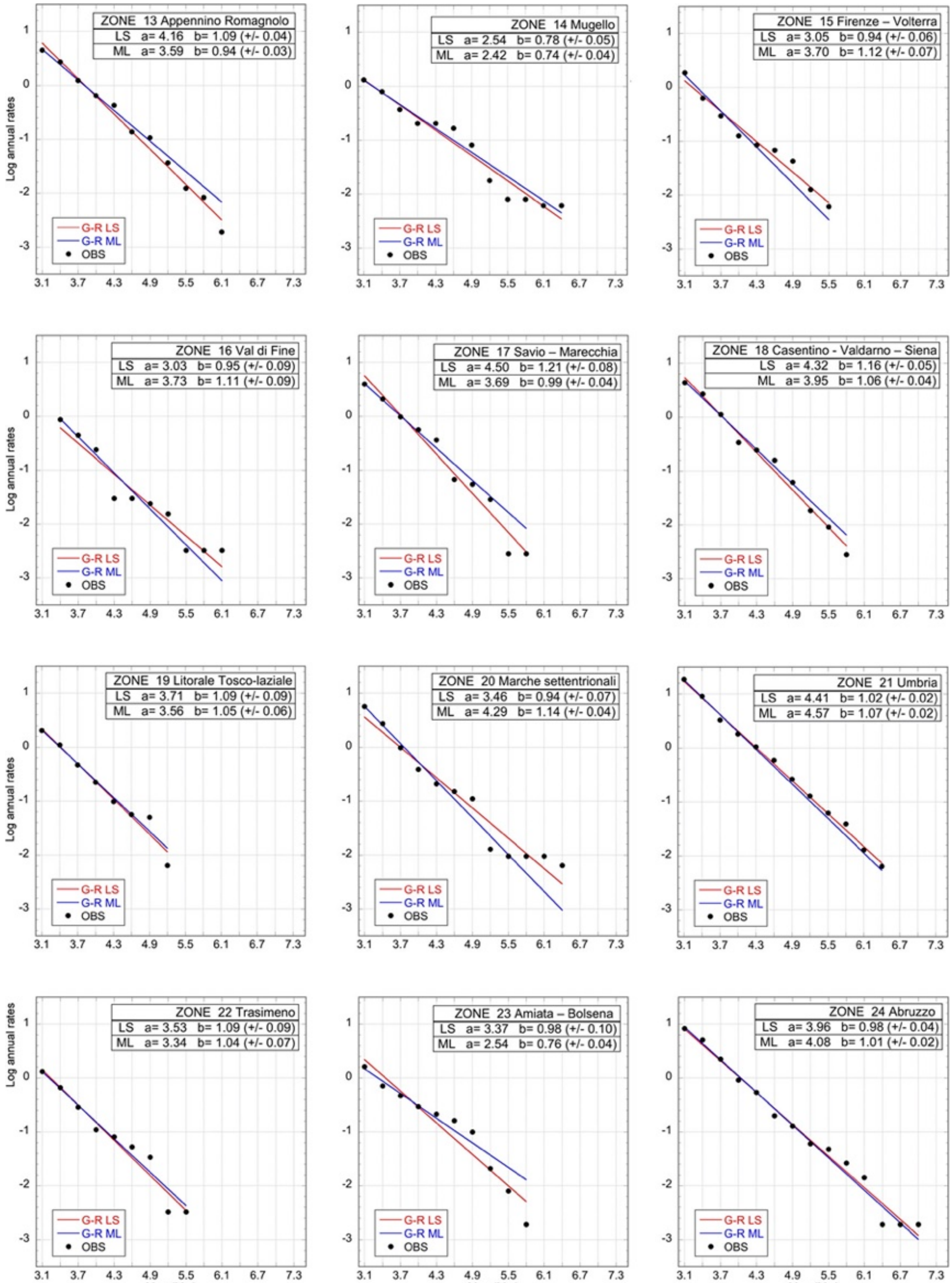

Fig. 4 (continued)

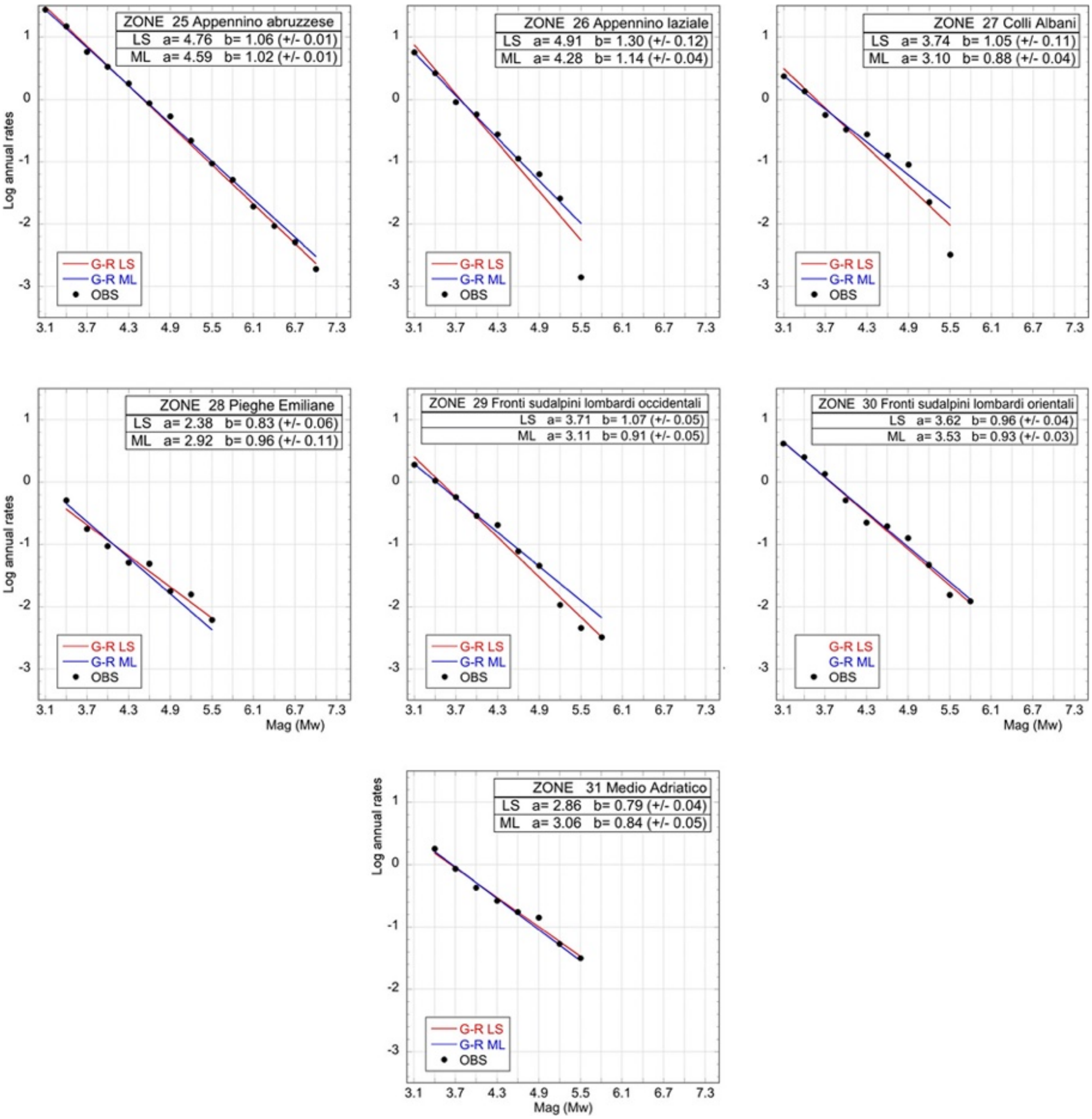

Fig. 4 (continued)

however, because the association of earthquakes to faults remains very problematic due to the uncertainties in earthquake location and the poor knowledge of the deep geometry of the faults.

To introduce in a simplified way the correct 3D geometry of the tectonic structures put into evidence by geological study, some inclined planes (seismogenic planes, SPs hereafter) have been designed inside each SZ. Although these geometries are extremely rough because they simplify with a few inclined elements the totality of faults present in the SZ, this model mimics the tectonic style better than that based on horizontal SZs.

In the first application (Santulin et al. 2014), a single SP has been considered inside each SZ, and the sectors characterised by transcurrent activity have been modelled by a vertical plane of very limited width

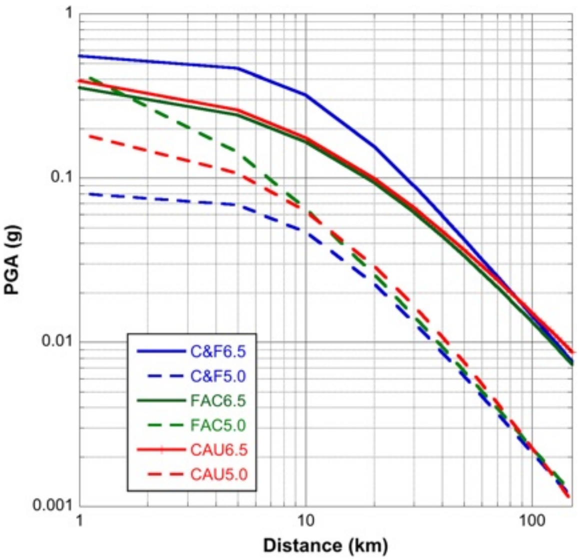

Fig. 5 Comparison among attenuation models: *C&F* Cauzzi and Faccioli (2008), *FAC* Faccioli et al. (2010), *CAU* Cauzzi et al. (2014). The C&F model considers the hypocentral distance, while both FAC and CAU models consider the rupture distance: both distances can be suitable for deep sources in the hazard computation and are equivalent to each other for $M_W \leq 5.7$ (Faccioli et al. 2010)

(3 km). This model has shown severe limitations as unrealistic depths have been reached for some SPs, assuming for them the dominant dip in the SZ and extending the SPs to cover the whole SZ.

Having a full geometric description available for the different SZs, a series of SPs has been designed inside each SZ (Fig. 7), obtaining in such a way a good approximation of the real tectonic scenario (Table 1). The superficial projection of the SPs generally covers the whole width of the SZ. Although this model is a simplification of a much more complicated reality, it surely mimics the tectonic setting of the study region. As some SZs are characterised by different fault styles, SPs of different rupture type (normal, reverse, strike-slip) have been designed. The geological characterisation of each SZ (Table 1) that identifies the different fault types present also has driven the percentage of activity (number of earthquakes) relevant to each SP (when more than one are present in the same SZ): the GR distribution of seismicity has been partitioned accordingly.

The new seismic hazard maps (Fig. 8) have been calculated taking into account all of the tectonic features pinpointed by the new seismogenic zonation (Martelli et al. 2014): each SZ is modelled by a suite of SPs, each of which is defined by a 3D geometry and an associated tectonic style. For each SP, the CAU GMPE relating to the tectonic style of that SP has been associated as an attenuation model for the ground shaking. The ground motion has been computed again for the four previously cited RPs: 101, 475, 950 and 1950 years.

Figure 8 shows the influence of the deep geometry of the SPs and their tectonic styles: the high expected ground motion for a 101-year RP (Fig. 8a) is located along the Northern Apennines margin with the maximum values (now 0.175 to 0.20 g) again in the SZ Romagna Apennines (No. 13 in Fig. 3 and Table 1). The SZ Emilia Apennines to the NW and the SZ Savio-Marecchia to the SE (No. 7 and No. 17, respectively, in Fig. 3 and Table 1) also show strong shaking (between 0.15 and 0.175 g). In addition, the areas adjacent to those with large PGA (Garfagnana, Romagna Margin and Ferrara Folds, Nos. 8, 12 and 3, respectively, in Fig. 3 and Table 1) and the Central Apennines to the south (SZs Umbria and Abruzzo, Nos. 21 and 25 in Fig. 3 and Table 1) are characterised by a PGA between 0.15 and 0.175 g. It is worthy to note the relatively low hazard estimated for the SZ Marche (No. 20 in Fig. 3 and Table 1) and, in addition, the minimum values found in the SZ Florence-Volterra, Tusco-Latium Littoral and Trasimeno areas (Nos. 15, 19 and 22 in Fig. 3 and Table 1). The similarity of the maps referring to different RPs is not surprising, as the application of a constant b-value implies a proportionality in the computed hazard. It is interesting to point out that strong shaking (PGA larger than 0.30 g for a 1950-year RP, see Fig. 8d) is also expected along the SZs Ferrara Folds and Adriatic Folds (Nos. 3 and 4 in Fig. 3 and Table 1) along the Adriatic coast.

A comparison between the results obtained considering classical SZs (Fig. 6) and those with inclined SPs (Fig. 8) shows that the areas with the strongest expected shaking remain the same, but the inclined SPs indicate a stronger shaking. Moreover, the use of SPs brings a more detailed definition of the expected ground motion and, consequently, a suite of small areas with a high PGA.

An additional elaboration has been performed for some specific sites, for which the uniform hazard response spectra (UHRSs) for a 475- and a 1950-year RP have been computed and compared with the related design spectra of the Italian building code (NTC 2008). The selected sites (see the locations in Fig. 3) coincide with important towns (Ancona, Bologna, Florence, Genoa, L'Aquila and Perugia) and Mirandola, which was involved in the seismic sequence of 2012. The shape of

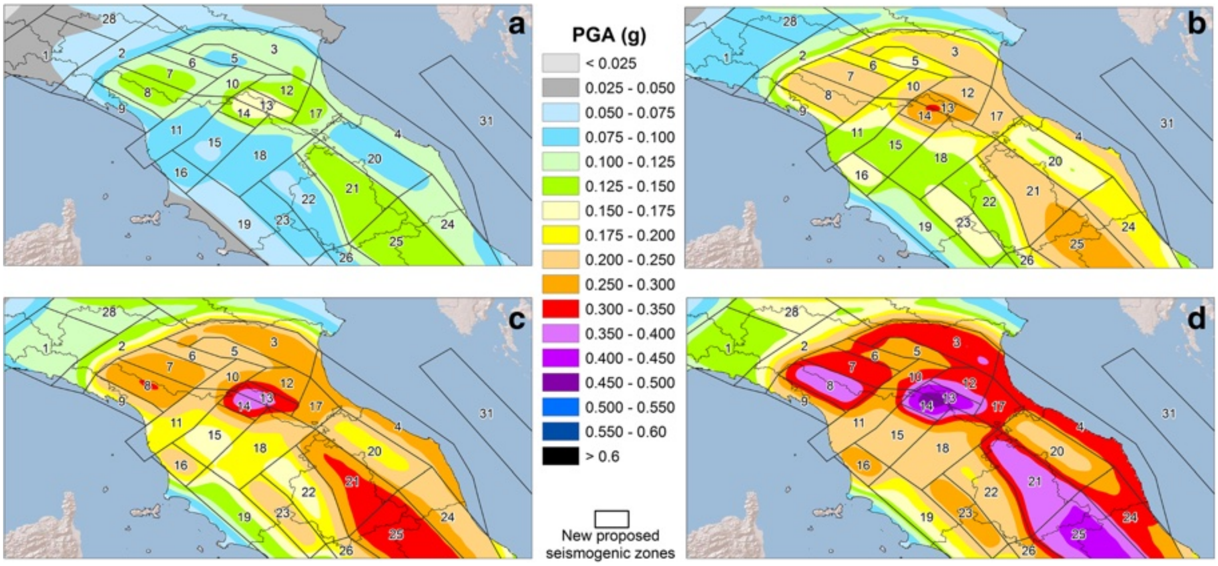

Fig. 6 PGA computed with the new seismogenic zonation treated in a superficial plane fashion: **a** 101-year RP; **b** 475-year RP; **c** 950-year RP; **d** 1950-year RP

the UHRSs is strongly conditioned by the GMPE applied in the computation; in the case of the CAU model, the biggest acceleration peaks strongly at 0.1 s without any flat top. Considering both RPs (Fig. 9), L'Aquila shows the largest hazard, while Genoa displays the lowest one, in both elaborations. When we compare the UHRSs of our elaboration with the design spectra of the Italian building code (NTC 2008), we see that only in the case of Genoa, the UHRSs for both 475- and 1950-year RPs remain inside the design spectra of the building code and that of Florence exceeds the design spectra only marginally at 0.1 s, especially for the 475-year RP. In all other cases, the high peak at 0.1 s is larger than the acceleration expected by the building code; in the case of Mirandola, in particular, the UHRS peak is almost double for both

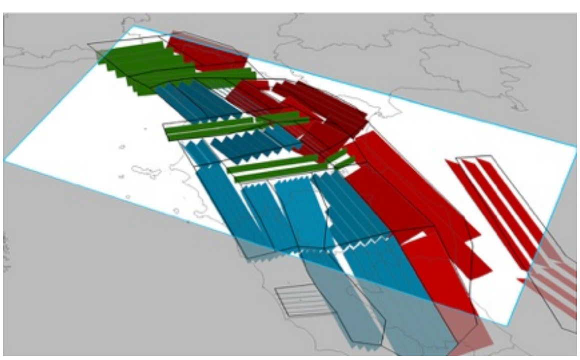

Fig. 7 3D seismogenic model for the Northern Apennines. The seismogenic sources are modelled as inclined planes (seismogenic planes, SPs)

RPs (see Fig. 9a, b). Apart from the peak at 0.1 s, for all other periods, the computed UHRSs are well below those of the Italian building code (NTC 2008). It is worth noting that the high acceleration at 0.1 s is a peculiarity of the attenuation model (Cauzzi and Faccioli 2008; Faccioli et al. 2010; Cauzzi et al. 2014) considered in the present elaboration.

4 Comparisons with previous hazard estimates

This new seismogenic zonation sounds quite innovative, especially for the introduction of inclined planes in seismic hazard computation coupled with a proper GMPE (that considers the rupture distance). But what is the actual difference in terms of expected ground shaking if comparisons are made to the standard maps that consider plane sources? The preliminary answer is given simply by the comparison between our estimates in Figs. 6 and 8, already described, which show greater detail produced by the inclined SPs.

To further investigate this aspect, a comparison with the values of the Italian seismic hazard map (hereafter MPS04; Gruppo di Lavoro 2004; Stucchi et al. 2011), based on the most recent national seismogenic zonation (hereafter ZS9; Meletti et al. 2008), which represents the basis of the official estimates of the Italian building code, has been produced for the 475-year RP. A strict comparison on the influence of the 2D geometry of the

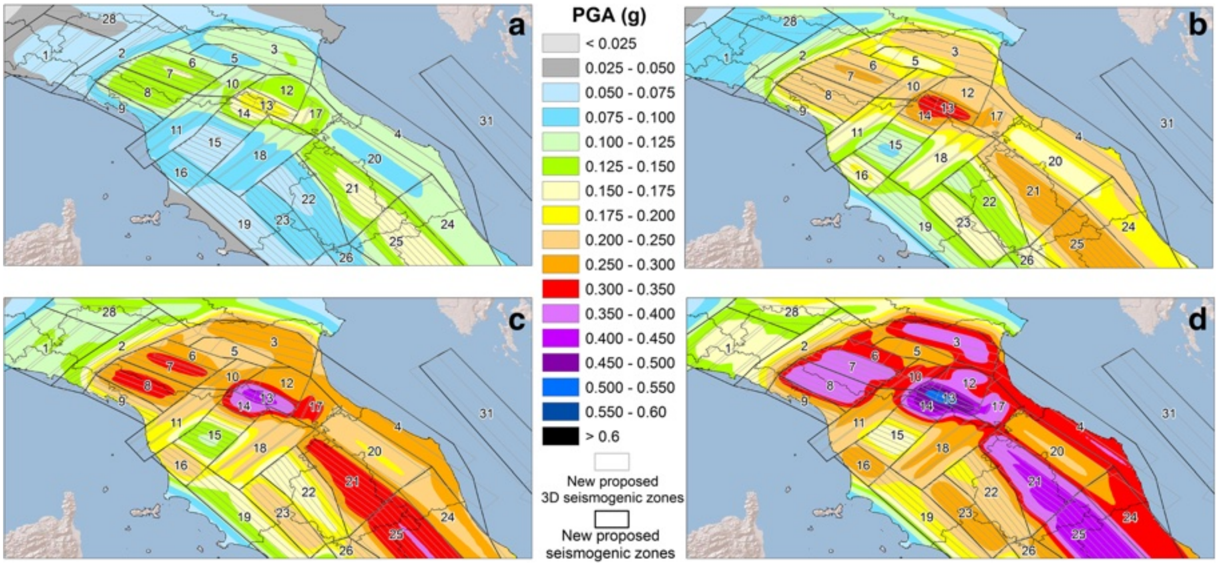

Fig. 8 PGA computed with the new seismogenic zonation using inclined dipping planes (SPs): **a** 101-year RP; **b** 475-year RP; **c** 950-year RP; **d** 1950-year RP

zonation is possible only in terms of plane sources with differentiated fault kinematics considering the same earthquake catalogue and the same GMPE. The expected ground motion computed with the new seismogenic zonation (Martelli et al. 2014) is much more articulated (Fig. 6b) than that of MPS04 (Fig. 10a) because of the more detailed zonation with narrower SZs, which sometimes concentrate the shaking. Conversely to MPS04 (Fig. 10a), where the largest hazard refers to the Central Apennines (corresponding roughly to ZS Abruzzo Apennines of the new zonation, No. 25 in Fig. 3 and Table 1), the new map (Fig. 6b) fixes the largest hazard in the Northern Apennines (SZs Romagna Apennines, No. 13 in Fig. 3 and Table 1), with similar values of PGA. These differences are clearly shown in Fig. 11, where the estimates obtained with both the plane and inclined sources are considered. In the case of plane sources (comparison between similar types of sources, Fig. 11a), the new map shows a slightly lower PGA than that in the MPS04 map only in SZ Taro Enza (No. 2 in Fig. 3 and Table 1); conversely, a higher ground motion is expected in almost all SZs where the largest values have been found in the new map, i.e. SZs Ferrara Folds, Emilia and Romagna Apennines, Mugello, and, for a limited portion, Umbria and Abruzzo (Nos. 3, 7, 13, 14, 21 and 25 in Fig. 3 and Table 1). A rather similar result, but with an emphasised impact on the SZs Ferrara Folds and Romagna Apennines (Nos. 3 and 13 in Fig. 3 and Table 1), is obtained when also considering inclined sources (Fig. 11b).

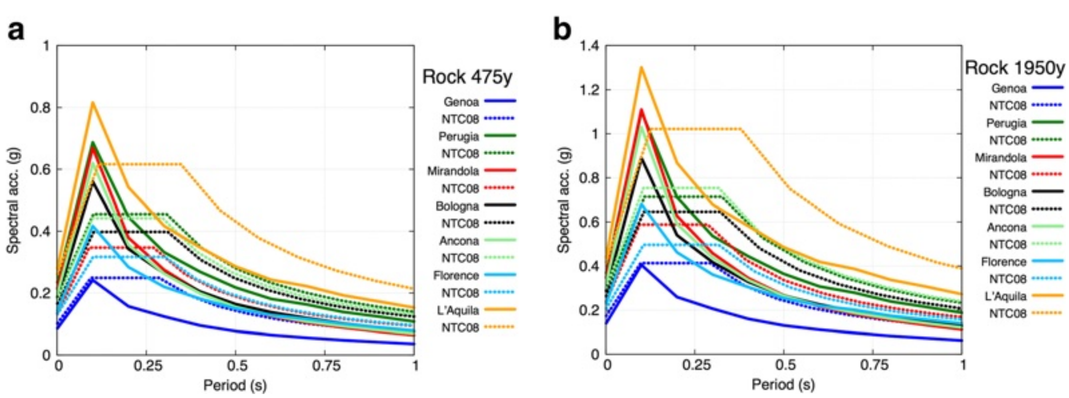

Fig. 9 UHRSs for the main towns in the study region: **a** 475-year RP; **b** 1950-year RP

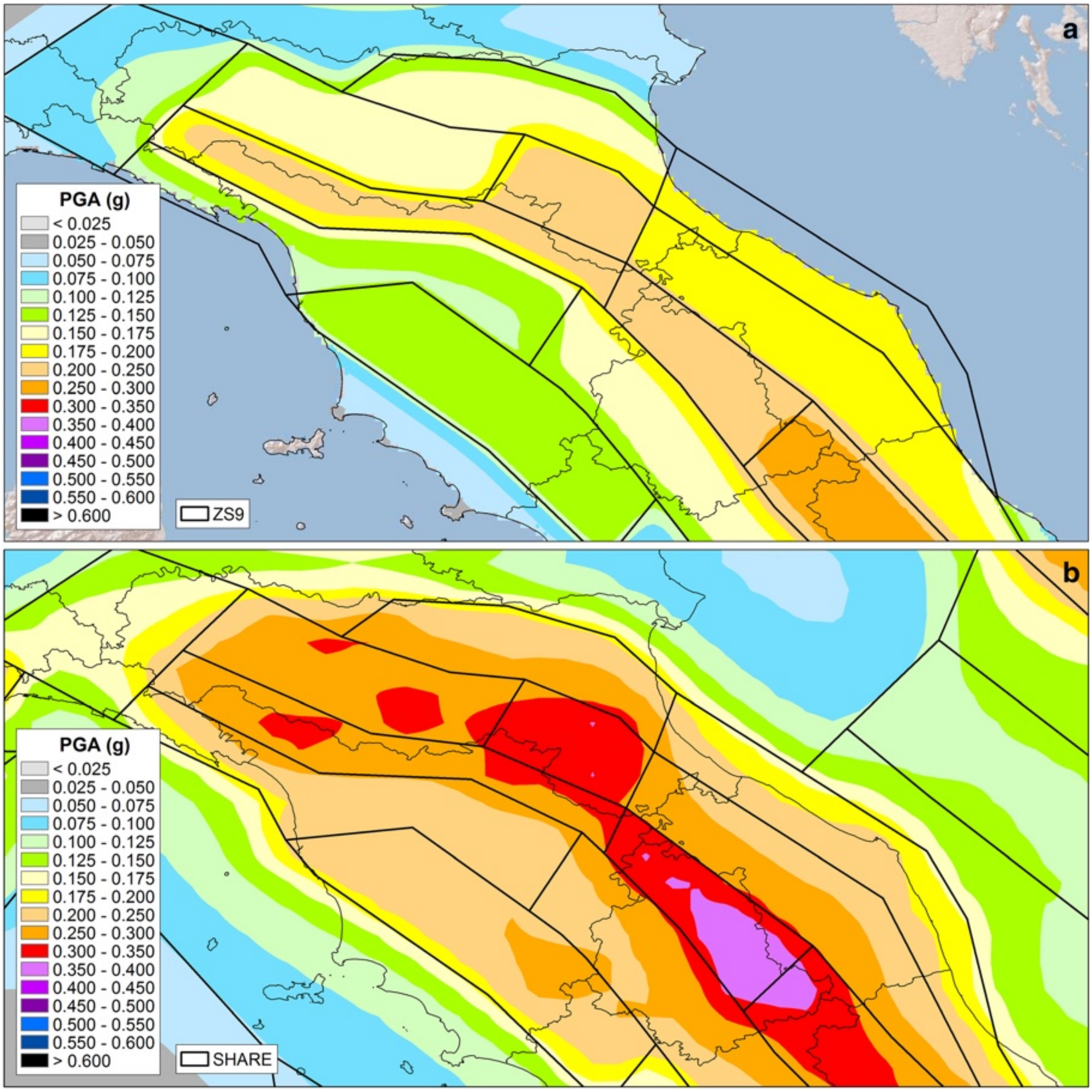

Fig. 10 PGA with a 475-year RP: **a** original MPS04 map; **b** original SHARE map (see the text for details)

An additional comparison has been established with the European seismic hazard map developed in the framework of the SHARE project (Giardini et al. 2013) where an articulated logic tree was considered for several parameters, among which zonation and GMPE (see Slejko et al. 2014). The resulting map (Fig. 10b) shows a wide area with an expected PGA of between 0.2 and 0.3 g covering a large part of the Emilia-Romagna region. The differences between the two maps (compare Figs. 6b and 10b) occur in several sectors of the study region, and the areas with the largest PGA values differ slightly. In general, we can say that the expected ground motion for a 475-year RP differs on average by 0.1 g. It is worth noting that the largest hazard of the SHARE map is located in the Central Apennines, while in the new map, the large ground motions are expected in the Northern Apennines.

The map with the final results of the present study, i.e. the map considering 3D inclined planes (Fig. 8b), displays slightly higher hazard than that with 2D horizontal planes (Fig. 6b), as already noted and explained. The map with

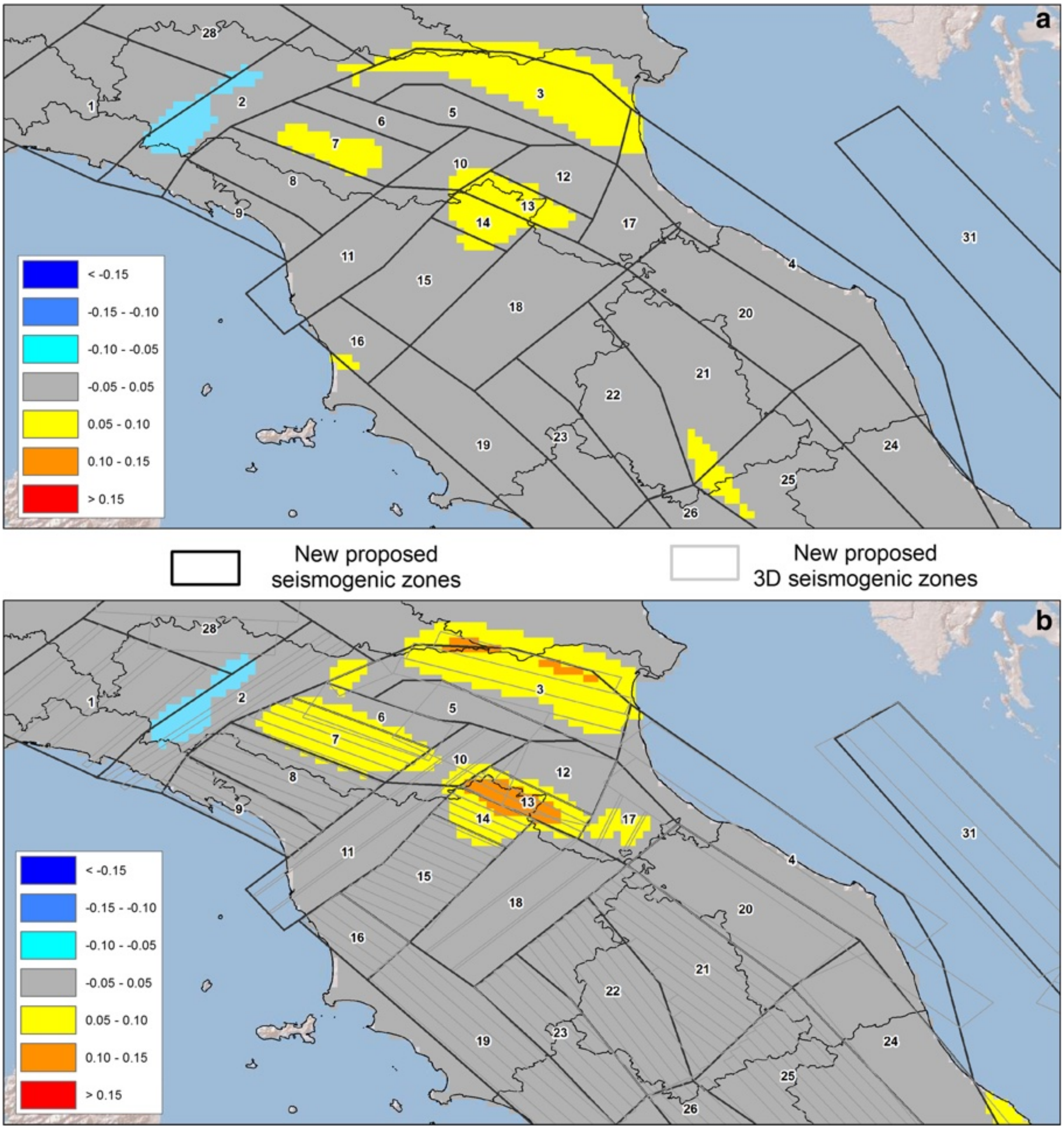

Fig. 11 Comparison between the new hazard estimates and those of MPS04 (PGA new map—PGA MPS04): **a** plain sources; **b** inclined sources

the 3D seismogenic model shows PGA values that are relatively close to that of the original MPS04 (Fig. 10a).

5 Conclusions

The application to the seismic hazard estimates of the new seismogenic zonation proposed for the Northern Apennines represents, in our opinion, a step forward in modelling seismogenic sources. The adopted inclined sources, here defined as SPs, are more detailed than the usual horizontal surfaces (SZs) but more general than the individual faults. In addition, they overcome the dilemma regarding the applicability of a characteristic earthquake model for the Italian tectonic context, because the GR seismicity model is more suitable for including several faults within each source as seems appropriate in this case.

The main novelties of the proposed zonation include the following:

- a division of some very large zones of ZS9 [e.g. SZs 912, 915, 916, 921 of Meletti et al. (2008)], which in our opinion included seismogenic structures with different geometry and failure mechanisms;
- the introduction of new SZs, including areas until now not considered seismogenic, such as some sectors of the central Po Plain and the Tyrrhenian coast;
- the introduction of transversal SZs motivated by the presence of Quaternary structures oriented approximately NE-SW, with strike-slip component, which deform structures oriented NW-SE.

The new hazard maps of the Northern Apennines (Fig. 8) show the high level of hazard along the Apennine chain with the strongest expected shaking located in the SZ Romagna Apennines and in part of the SZ Mugello (Nos. 13 and 14 in Fig. 3 and Table 1) and with values larger than 0.30 g for a 475-year RP, and to a lesser extent in the SZs Emilia Apennines, Mugello, Savio-Marecchia, Umbria and Abruzzo (Nos. 7, 14, 17, 21, 25 in Fig. 3 and Table 1). The computed UHRSs for the main towns in the studied region pinpoint that hazard is high in L'Aquila and low in Genoa and Florence.

Appendix. Description of the seismogenic zones

1 Liguria: This zone corresponds to zone 911 of the ZS9, but trimmed in the northern sector (which was included in the previous zone); it maintains the main seismotectonic features of zone 911 of ZS9 (Meletti et al. 2008), with dominant strike-slip faulting along transverse structures and maximum observed M_W≈5.7. The seismogenic sources in this zone have been reproduced by assuming four planes trending NE-SW and dipping at ~90°, with strike-slip kinematics.

2 Taro-Enza: The zone is characterised by important NE-SW transverse strike-slip structures that cross the Apennines chain, connecting the Ligurian Sea to the Po Plain (Figs. 1 and 2). However, the P axis is roughly N-S oriented according to the local slip vector. Hypocentral depths may be high (>30 km) and the historical maximum M_W is ≈5.5. This zone corresponds to the western part of zones 913, 915 and 916 of ZS9. This zone has been modelled by considering strike-slip faulting on two planes trending NE-SW and dipping at ~90°.

3 Ferrara Folds: In this zone, we have included the entire external front of the Ferrara folds with similar tectonic features of the 912 zone of ZS904: compressive kinematics with P axes oriented N-S along 45° south-dipping thrust faults. Hypocentral depths range between 5 and 15 km, and the maximum M_W is 6.1, registered during the May 2012 seismic sequence. This zone is part of the ZS9 912 zone, which has been subdivided, creating a new zone (5 in Fig. 2) that is characterised by minor density and intensity of earthquakes and scarce evidence of active structures in the field. The seismogenic sources in this area have been modelled by considering four planes, dipping to the S-SSW at ~45° with thrust-fault kinematics.

4 Adriatic Folds: This zone corresponds in the ZS9 to zone 917 with dominant active thrusts (Meletti et al. 2008). Geomorphologic evidence suggests the presence of active growing anticlines along the Adriatic coast (Vannoli et al. 2004). Historical maximum magnitude is M_W≈6.1. This area has been modelled by assuming thrust faulting on two planes dipping to the S-SSW at ~30°.

5 Nonantola-Budrio: The zone is located between zone 3 and the Pede-Apennine margin. It is characterised by low seismicity and scarce evidence of active structures. It corresponds to the southern 912 zone of ZS9. The expected earthquakes should have compressive kinematics along low-angle south-dipping planes that are likely coincident with the flats of the thrusts of zone 3. Depth is expected between 10 and 35 km, with P axes roughly N-S oriented. Historical maximum magnitude is M_W≈5.5. This zone has been modelled by assuming a single plane dipping to the SW at ~20° with thrust kinematics.

6 Emilia Margin: This zone corresponds to the central sector of zone 913 of ZS9 and it is characterised by numerous geologic evidence of recent and active tectonics mainly related to the Pede-Apennine thrust. Moderate to strong earthquakes show compressive kinematics with P axes trending N-S and associated to south, 45°–60° dipping thrust fault. Hypocentral depths range between 10 and 30 km.

Historical magnitude is ≈6. The deformation in this zone has been modelled by assuming a single S-dipping plane with inclination of ~45°–60° and thrust faulting.

7 Emilia Apennines: This zone shows minor-intensity earthquakes but with two different kinematics: compressive with hypocentral depth of 15–35 km, with P axes trending N-S, and shallower (5–15 km) extensional events. The maximum historical magnitude is ≈5.5. Zone 7 corresponds to the southern part of zone 913 of ZS9. The seismogenic sources in this area have been modelled by considering normal faulting events on four planes, dipping to the N at ~60°.

8 Garfagnana: This zone includes the Lunigiana and Garfagnana basins (Fig. 1) and shows frequent and strong earthquakes (M>6). It also includes part of the Apennines divide area. Main active faults dip either to the SW or to the NE and show extensional kinematics. Transtensional, right-lateral transverse structures trending NE-SW to NNE-SSW are also present. Hypocentral depths are mainly concentrated in the range between 5 and 15 km, with a maximum historical magnitude of ≈6.5 associated with the Garfagnana 1920 event. Zone 8 coincides with the western part of zone 915 of ZS9. This zone has been modelled by assuming five NW-SE-trending planes with normal fault kinematics. Three planes dip to the SW, whereas 2 planes dip to the NE; the dip of all these planes is ~65°.

9 NW Coastal Sector: This zone is cut along the Tyrrhenian coast and shows low intensity and rare seismic activity. Quaternary, potentially active faults are normal and mainly dip to the SW. Hypocentral depths range between 5 and 15 km and a maximum historical M_W≈5.4 has been recorded in the area. This zone includes the coastal sectors of 916 zone of ZS9. The seismogenic sources in this area have been modelled by assuming normal faulting events on four planes, dipping to the SW at ~65°.

10 Reno-Setta: This zone extends from the divide to the Apennine margin in the Bologna area (Figs. 1 and 2). It has a lower frequency and intensity of seismic events with hypocentral depth ranging between 5 and 35 km. The active or potentially active structures are generally transverse to the chain; along the Apennine margin, active compressive structures strongly dipping (45°–60°) to the south, may also occur. Associated to the registered events is a P axis trending N-S, with hypocentral depth of between 15 and 35 km. Historical magnitude is M_W≈5.5. Zone 10 corresponds to the eastern sector of zone 913 of ZS9. This zone has been modelled by assuming strike-slip deformation on two subvertical (dip ~90°) planes trending NNE-SWW.

11 Pistoia-Pisa: This transverse zone includes the Pisa plain, the southern part of Garfagnana basin and the western sector of the Florence basin up to the Apennines divide. Active or potentially active structures trend NE-SW, but they usually do not show clear kinematics. Minor NW-SE-trending SW-dipping normal faults are also present. Hypocentral depths range between 5 and 15 km, and the historical maximum magnitude is M_W≈5.7. Zone 11 coincides with central parts of 915 and 916 and the northern sector of 921 of the ZS9 zones. This zone has been modelled by assuming two subvertical (dip ~90°) planes trending NE-SW with strike-slip kinematics.

12 Romagna Margin: This zone includes another sector of the Apennines margin in an area characterised by frequent and strong earthquakes associated with active, south dipping (30–45°) thrust faults with sub-horizontal ≈N-S-trending P axes. Hypocentral depth usually ranges between 10 and 25 km, but deeper events (up to 35 km) are also present. The historical maximum magnitude is M_W≈6.1. Zone 12 approximately corresponds to the northern portion of the 914 zone. Deformation in this area has been modelled with a single plane source dipping to the S at ~30–45° and thrust faulting.

13 Romagna Apennines: This zone shows frequent and high-intensity earthquakes with hypocentral depths of 15 and 20 km generally associated to south-dipping thrust faults. Rare transcurrent kinematics have also been registered. Shallower (<10 km) events have been registered associated to NW-SE-striking, NE-dipping normal faults. The historical maximum magnitude is M_W≈6. Zone 13 approximately corresponds to the southern portion of the 914 zone. Calculations in this zone have been performed by considering three NE-dipping planes, with inclination of ~65° and normal fault displacement.

14 Mugello: This zone shows frequent and high-intensity seismic events. It largely corresponds to the Mugello basin area, where well-developed

active and potentially active faults have been documented. Most of these structures show extensional kinematics. They are generally NW-SE striking, and dip either to the SW or to the NE. At the NW and SE ends of the Mugello basin, tranverse NE-SW-trending structures are present, although their kinematics are not yet well defined. Hypocentral depths of the registered events are usually in the 5–15 km range, and the historical maximum magnitude is M_W≈6.3, associated with a 1919 earthquake. Zone 14 corresponds to the eastern part of 915 zone of the ZS9. This zone has been modelled by assuming normal faulting on four planes, two dipping to SSW and two dipping to the NNE at ~65°.

15 Florence-Volterra: This wide zone includes the central northern area of Tuscany up to the Florence basin, which is characterised by NW-SE-trending and SW-dipping active normal faults. Subordinately NE-SW-trending (transverse) transcurrent faults are also present with dextral and sinistral kinematics. Hypocentral depths are in the range of 5 to 15 km, and the historical maximum magnitude is M≈5.4 and has been associated with an 1895 earthquake whose epicentre was located 10 km south of Florence. This zone includes the central-eastern sector of the 916 zone and part of the northern area of zone 921 of the ZS9. Calculations in this zone have been performed by considering ten planes, dipping to the SW at ~65° and normal fault displacement.

16 Val di Fine: This small zone encompasses a sector of the Tuscan coast where it is likely that the strong earthquake of August 14, 1846, for which a magnitude of M_W≈5.91 has been inferred, was located. The zone is included in the northern sector of zone 921 of the ZS9. The active structures responsible for this event were the NNW-SSE- striking normal faults delimiting the eastern side of the Fine Basin (Figs. 1 and 2). Hypocentral depths can likely be located between 5 and 15 km. Deformation in this area has been modelled with four planes, dipping to the WSW at ~65° and characterised by normal faulting.

17 Savio-Marecchia: This area is located along the external margin of the chain and reaches the main divide. It is characterised by transverse structures with strike-slip kinematics as well as by thrust faults with N-S-oriented P axes, more frequently along the Apennine margin. Hypocentral depths are between 5 and 15 km for the transversal structures, 15 and 25 km along the southern-dipping thrust faults. Historical maximum magnitude is M_W≈6.0. This zone includes the south-eastern sectors of 914 and 915 zones, and the north-western parts of the 918 and 919 zones of the ZS9. This zone has been modelled by assuming strike-slip faulting on two planes, trending NNE-SSW and dipping at ~90°.

18 Casentino-Valdarno-Siena: This is a wide transverse zone running between central Tuscany (Siena basin) up to the Apennines divide (Casentino basin). Main active and potentially active structures trend NE-SW, likely with a dextral transtensional component. Normal faults oriented NW-SE oriented and dipping SW are also present. Hypocentral depths have been located between 5 and 15 km, and the maximum historical magnitude is M_W≈5.8. This zone corresponds to the external sectors of 915 and 916 in the ZS9, to the north-western sector of zone 920 and to the central sector of zone 921. This zone has been modelled by assuming strike-slip deformation on two subvertical (dip ~90°) planes trending NE-SW.

19 Tusco-Latium Littoral: This zone, not previously included in the ZS9, encompasses a sector of the hinterland of Tuscany close to the Tyrrhenian coast (Figs. 1 and 2). A few potentially active normal faults are oriented NW-SE and associated with transversal NE-SW-trending strike-slip and normal faults. Part of the seismicity of the area is related to the Larderello Geothermal field (Fig. 1). Hypocentral depths are between 5 and 15 km, and the maximum historical magnitude is M_W≈5.1. Deformation in this area has been modelled with four planes, dipping to the SW at ~60° and characterised by normal faulting.

20 Marche North: This zone coincides with zone 918 of the ZS9, but modified in its north-western part and cut in half to allow for zone 24 (see below). This zone is affected by many seismic events, including of high intensite. Active structures are essentially SW-dipping thrust faults. Hypocentral depths have been located at between 10 and 35 km, and the maximum historical magnitude is M_W≈6.4. Calculations in this zone have been performed by using a single plane source dipping to the SW at 30° and thrust faulting.

21 Umbria: This zone is characterised by frequent and high-intensity seismicity. The main active structures are W- and SW-dipping normal faults. In the southern sector NNE-SSW-trending dextral transtensional faults have been detected. Hypocentral depths are between 5 and 15 km, and the maximum historical magnitude is M_W≈6.7. This zone corresponds to ZS9 919, although slightly modified in the north-western and south-eastern limits. This zone has been modelled by assuming normal faulting on nine planes, five of which dip to the SW and four to the ENE; the inclination is assumed at ~65°.

22 Trasimeno: This zone corresponds partially to the northern sector of zone 920 of ZS9. Few seismic events, of low to medium intensity, occur in this area. Evidence of active or potentially active structures has not been found in the field. The maximum historical magnitude is M_W≈5.0. Deformation in this area has been modelled with six planes, dipping to the WSW at ~65° and characterised by normal faulting.

23 Amiata-Bolsena: This zone includes the Amiata Volcano and the northern part of the Roman magmatic province, including Lake Bolsena (Figs. 1 and 2). It corresponds to the south-western part of zone 921 of the ZS9. A few Quaternary and potentially active faults have been identified with extensional kinematics. Hypocentral depths are between 5 and 15 km, and the maximum historical magnitude is M_W≈5.7. Calculations in this zone have been performed by assuming normal faulting on four planes, dipping to the WSW at ~65°.

24 Abruzzo: This zone is located in the external part of the Apennines and it is characterised by medium-frequency and -intensity seismic events. Seismogenic structures are essentially SW-dipping thrust faults. Hypocentral depths have been located mainly between 10 and 35 km, and the maximum historical magnitude is M_W≈5.5. This zone corresponds to the southern part of zone 918 of the ZS9. Deformation in this area has been modelled with a single plane, dipping to the SW at ~30° and characterised by thrust faulting.

25 Abruzzo Apennines: This zone essentially corresponds to zone 923 of the ZS9, slightly modified in its north-western limits. The zone is affected by high-frequency and -intensity seismicity associated with active normal faults that are mainly SW-dipping. Hypocentral depths are generally in the range of between 5 and 15 km, and the maximum historical magnitude is M_W≈7.1, associated with the Fucino earthquake of 1915. The zone also includes the area where on April 2009 a 6.3 earthquake struck the town of L'Aquila (Figs. 1 and 2). Deformation in this area has been modelled by assuming normal faulting on nine SW-dipping planes, with inclination of ~65°.

26 Latium Apennines: This zone mainly coincides with the southern part of zone 920 of ZS9. The dominant kinematics of the seismicity is extensional, with maximum historical magnitude M_W≈5.5 (Meletti et al. 2008). This zone has been modelled by assuming normal faulting on five planes, dipping to the SW and with an inclination of ~65°.

27 Alban Hills: This SZ corresponds to zone 922 of the ZS9 and is centred in the Alban Mountains. It is characterised by seismicity associated with the activity of normal faults, oriented NE-SW and dipping NW, as documented in the DISS 3.2 (Basili et al. 2008; DISS Working Group 2015). As such, deformation in this area has been modelled by assuming six planes, dipping to the NW at ~65° and characterised by normal faulting.

28 Emilia Folds: This zone includes the western Emilia folds and Pede-Apennine thrust front, where strike-slip movements were also recognised. The main seismogenic structures are thrusts dipping 45° towards the south; the compression direction (P-axis) is around N-S. Hypocentral depths of the instrumental events are variable between 5 and 30 km. The maximum historical magnitude is M_W=5.5. The northern part of this area was not included in any ZS9 area, the southern part was the northern sector of zone 911 of the ZS9. Calculations in this zone have been performed by using seven plane sources dipping to the SW at 30° and thrust faulting.

For the calculation of the seismic hazard (see Chapter 3), in addition to the SZs described above, it was necessary to consider other SZs, that could influence the seismic hazard in the study area:

29 Western Lombard Southern Alpine Margin: This zone corresponds to zone 906 of the ZS9, modified to include the main western events and the thrust

fronts of the Lombard Southalpine margin. It maintains the same seismotectonic features as zone 906 (Meletti et al. 2008), i.e. south-verging thrust deformation along active faults dipping to the north. Calculations in this zone have been performed by using a single source dipping to the N at 30° and thrust faulting.

30 Eastern Lombard Southern Alpine Margin: This zone corresponds to zone 907 of the ZS9, modified to include the main western events and the thrust fronts of the Lombard Southalpine margin. It maintains the same seismotectonic features as zone 907 (Meletti et al. 2008), i.e. S-verging thrust deformation along active faults dipping to the north. Deformation in this area has been modelled by assuming a single thrust fault, dipping to the N at ~30°.

31 Middle Adriatic: This zone includes major earthquakes in the central Adriatic Sea. This area was not included in ZS9. The seismogenic structures are thrusts dipping to the E-NE at 45°, with hypocenter depths between 5 and 15 km. The maximum expected magnitude is $M_W \approx 6$. This zone has been modelled by assuming thrust faulting on seven planes, dipping to the E and with an inclination of ~30°.

References

Amato A, Cimini GB (2001) Deep structure from seismic tomography. In: Vai GB, Martini IP (eds) Anatomy of an Orogen: the Apennines and adjacent Mediterranean basins. Kluwer Academic Publishers, Boston, pp 33–45

Barberi F, Scandone P (eds) (1983) Structural model of Italy, scale 1:500,000. Progetto Finalizzato Geodinamica. Consiglio Nazionale delle Ricerche, Rome

Basili R, Valensise G, Vannoli P, Burrato P, Fracassi U, Mariano S, Tiberti MM, Boschi E (2008) The database of individual Seismogenic sources (DISS), version 3: summarizing 20 years of research on Italy's earthquake geology. Tectonophysics 453:20–43

Benedetti LC, Tapponnier P, Gaudemer Y, Manighetti I, Van der Woerd J (2003) Geomorphic evidence for an emergent active thrust along the edge of the Po plain: the Broni–Stradella fault. J Geophys Res 108:22–38 http://dx.doi.org/10.1029/2001JB001546

Boccaletti M, Guazzone G (1972) Gli archi appenninici, il Mar Ligure ed il Tirreno nelquadro della tettonica dei bacini marginali di retro-arco. Mem Soc Geol Ital 11:201–216

Boccaletti M, Elter P, Guazzone G (1971) Plate tectonic models for the develop-ment of the western alps and northern Apennines. Nature Physics Science 234:108–111

Boccaletti M, Coli M, Eva C, Ferrari G, Giglia G, Lazzarotto A, Merlanti F, Nicolich R, Papani G, Postpischl D (1985) Considerations on the seismotectonics of the northern Apennines. Tectonophysics 117:7–38

Boccaletti M, Bonini M, Corti G, Gasperini P, Martelli L, Piccardi L, Tanini C, Vannucci G (2004) Seismotectonic map of the Emilia–Romagna region, Scale1:250,000, with explanatory notes. SELCA Società Elaborazioni Cartografiche, Florence

Boccaletti M, Calamita F, Viandante MG (2005) La Neo-Catena litosferica appenninica nata a partire dal Pliocene inferiore come espressione della convergenza Africa-Europa. Boll Soc Geol It 124:87–105

Boccaletti M, Corti G, Martelli L (2011) Recent and active tectonics of the external zone of the northern Apennines (Italy). Int J Earth Sci (Geologische Rundschau). doi:10.1007/s00531-010-0545-y

Bonini M (1999) Basement-controlled Neogene polyphase cover thrusting and basin development along the Chianti Mountains ridge (northern Apennines, Italy). Geol Mag 136:133–152

Bonini M (2013) Fluid seepage variability across the external northern Apennines (Italy): structural controls with seismotectonic and geodynamic implications. Tectonophysics 590:151–174 http://dx.doi.org/10.1016/j.tecto.2013.01.020

Bonini M, Sani F, Stucchi EM, Moratti G, Benvenuti M, Menanno G, Tanini C (2014) Late Miocene shortening of the northern Apennines back-arc. J Geodyn 74:1–31

Brogi A, Liotta D (2008) Highly extended terrains, lateral segmentation ofthe substratum, and basin development: the middle-late Miocene Radi-condoli Basin (inner northern Apennines, Italy). Tectonics 27:TC5002. doi:10.1029/2007TC002188

Carminati E, Lustrino M, Doglioni C (2012) Geodynamic evolution of the central and western Mediterranean: tectonics vs. igneous petrology constraints. Tectonophysics 579:173–192

Cassinis R, Scarascia S, Lozej A (2005) Review of seismic wide-angle reflection-refraction (WARR) results in the Italian region (1956–1987). Chapter 2 –lithospheric tectono-stratigraphic setting of the Ligurian Sea – northern Apennines – Adriatic foreland from integrated CROP seismic data. In: Finetti I (ed) CROP project – deep seismic exploration of the Central Mediterranean and Italy, Atlases in geoscience, vol 1. Elsevier BV. ISBN 0-444-50693-4, Amsterdam, pp 31–55

Castellarin A, Eva C, Giglia G, Vai GB (1985) Analisi strutturale del Fronte Appenninico Padano. Giorn Geol 47:47–75

Castello B, Selvaggi G, Chiarabba C, Amato A (2006) CSI Catalogo della sismicità italiana 1981–2002, versione 1.1. INGV-CNT, Roma, <http://csi.rm.ingv.it>

Cauzzi C, Faccioli E (2008) Broadband (0.05 to 20 s) prediction of displacement response spectra based on worldwide digital records. J Seismol 12:453–475

Cauzzi C, Faccioli E, Vanini M, Bianchini A (2014) Updated predictive equations for broadband (0.01-10 s) horizontal response spectra and peak ground motions, based on a global dataset of digital acceleration records. Bull Earthq Eng. doi:10.1007/s10518-014-9685-y

CEN (Comité Européen de Normalisation) (2002) Eurocode 8: design of structures for earthquake resistance. Part 1: general rules, seismic actions and rules for buildings. Draft No 5, Doc CEN/T250/SC8/N317, CEN, Brussels, 100 pp

Chiarabba C, Jovane L, Di Stefano R (2005) A new view of Italian seismicity using 20 years of instrumental recordings. Tectonophysics 395:251–268

Chiarabba C, Amato A, Anselmi M, Baccheschi P, Bianchi I, Cattaneo M, Cecere G, Chiaraluce L, Ciaccio MG, De Gori P, De Luca G, Di Bona M, Di Stefano R, Faenza L, Govoni A, Improta L, Lucente FP, Marchetti A, Margheriti L, Mele F, Michelini A, Monachesi G, Moretti M, Pastori M, Piana Agostinetti N, Piccinini D, Roselli P, Seccia D, Valoroso L (2009) The 2009 L'Aquila (central Italy) MW6.3 earthquake: main shock and aftershocks. Geophys Res Lett 36:L18308. doi:10.1029/2009GL039627

Chiarabba C, De Gori P, Mele M (2015) Recent seismicity of Italy: active tectonics of the central Mediterranean region and seismicity rate changes after the mw 6.3 L'Aquila earthquake. Tectonophysics 638:82–93. doi:10.1016/j.tecto.2014.10.016

Ciaccio MG, Chiarabba C (2002) Tomographic models and seismotectonies of the Reggio Emilia region, Italy. Tectonophysics 344:261–276

Collettini C, Boncio P, Lavecchia G, Ponziani F, Federico C (1997) Sismicità "profonda" e geometria delle deformazioni intra-litosferiche in Italia centrale. In: Atti XVI Convegno GNGTS. AIT-CDRom, Rome

Collettini C, Chiaraluce L, Pucci S, Barchi MR, Cocco M (2005) Looking at fault reactivation matching structural geology and seismology. J Struct Geol 27:937–942

Cornell CA (1968) Engineering seismic risk analysis. Bull Seism Soc Am 58:1583–1606

D'Agostino N, Jackson JA, Dramis F, Funiciello R (2001) Interactions between mantle upwelling, drainage evolution and active normal faulting: an example from the central Apennines (Italy). Geophys J Int 147:475–497

Della Vedova B, Bellani S, Pellis G, Squarci P (2001) Deep temperatures and surface heat flow distribution. In: Vai GB, Martini IP (eds) Anatomy of an Orogen: the Apennines and the adjacent Mediterranean basins. Kluwer Academic Publisher, Boston, pp 65–76

Di Bucci D, Mazzoli S (2002) Active tectonics of the northern Apennines and Adria geodynamics: new data and a discussion. J Geodyn 34:687–707

DISS Working Group (2015) Database of Individual Seismogenic Sources (DISS), Version 3.2.0: A compilation of potential sources for earthquakes larger than M 5.5 in Italy and surrounding areas. http://diss.rm.ingv.it/diss/, © INGV 2015 - Istituto Nazionale di Geofisica e Vulcanologia. DOI:10.6092/INGV.IT-DISS3.2.0

Doglioni C (1991) A proposal for the kinematic modeling of W-dipping subduction - possible applications to the Tyrrhenian-Apennines system. TerraNov. 3:423–434

Doglioni C, Mongelli F, Pialli G (1998) Boudinage of the Alpine belt in the Apenninicback-arc. Mem Soc Geol Ital 52:457–468

Doglioni C, Gueguen E, Harabaglia P, Mongelli F (1999) On the origin of west directed subduction zones and applications to the western Mediterranean. In: Durand B, Jolivet L, Horváth F, Séranne M (eds) The Mediterranean basins: tertiary extension within the Alpine Orogen, Special publications, vol 156. Geological Society, London, pp 541–561

Elter P, Giglia G, Tongiorgi M, Trevisan L (1975) Tensional and compressional areas in the recent (Tortonian to present) evolution of the northern Apennines. Bollettino di Geofisica Teorica e Applicata 17:3–18

Eva E, Solarino S (1992) Alcune considerazioni sulla simotettonica dell'Appennino nord-occidentale ricavate dall'analisi si meccanismi focali. Studi Geologici Camerti Spec 1992/2, Appendice CROP 1-1A:75–83

Faccenna C, Funiciello F, Giardini D, Lucente P (2001) Episodic back-arc extension during restricted mantle convection in the central Mediterranean. Earth Planet Sci Lett 187:105–116

Faccioli E, Bianchini A, Villani M (2010) New ground motion prediction equations for T>1 s and their influence on seismic hazard assessment. In: Proceedings of the University of Tokyo Symposium on long-period ground motion and urban disaster mitigation

Fantoni R, Franciosi R (2010) Tectono-sedimentary setting of the Po plain and Adriatic foreland. Rend Fis Acc Lincei 21(Suppl 1):S197–S209. doi:10.1007/s12210-010-0102-4

Finetti IR, Boccaletti M, Bonini M, Del Ben A, Pipan M, Prizzon A, Sani F (2005) Chapter 8 – lithospheric tectono-stratigraphic setting of the Ligurian Sea –northern Apennines – Adriatic foreland from integrated CROP seismic data. In: Finetti I (ed) CROP project – deep seismic exploration of the Central Mediterranean and Italy, Atlases in geoscience, vol 1. Elsevier BV, ISBN 0-444-50693-4, Amsterdam, pp 119–158

Galadini F, Galli P, Cittadini A, Giaccio B (2001) Late Quaternary fault movements in the Mt. Baldo-Lessini Mts. Sector of the Southalpine area (northern Italy). Geologie en Mijnbouw (Netherlands Journal of Geosciences) 80:119–140

Gardner JK, Knopoff L (1974) Is the sequence of earthquakes in southern California, with aftershocks removed, Poissonian? Boll Seism Soc Am 64:1363–1367

Gasperini P (ed) (2004) Catalogo dei terremoti CPTI2 - App.1 al Rapporto Conclusivo. Ist. Naz. Geofisica e Vulcanologia, Italy 29 pp

Giardini D, Woessner J, Danciu L, Crowley H, Cotton F, Grunthal G, Pinho R, Valensise G, Akkar S, Arvidsson R, Basili R, Cameelbeeck T, Campos-Costa A, Douglas J, Demircioglu MB, Erdik M, Fonseca J, Glavatovic B, Lindholm C, Makropoulos K, Meletti C, Musson R, Pitilakis K, Sesetyan K, Stromeyer D, Stucchi M, Rovida A (2013) Seismic hazard harmonization in Europe (SHARE): Online Data Resource. doi:10.12686/SED-00000001-SHARE

Gruppo di Lavoro (2004) Redazione della mappa di pericolosità sismica prevista dall'Ordinanza PCM 3274 del 20 marzo 2003. Rapporto conclusivo per il Dipartimento della Protezione Civile. INGV, Milano - Roma 65 pp + 5 App

ISIDe Working Group (2015) Database of seismic events of Italy (1981-present). Available from http://iside.rm.ingv.it

Kijko A, Graham G (1998) Parametric-historic procedure for probabilistic seismic hazard analysis. Part I: estimation of maximum regional magnitude mmax. Pure Appl Geophys 152:413–442

Lavecchia G, Boncio P, Creati N (2003) A lithospheric-scale seismogenic thrust incentral Italy. J Geodyn 36:79–94

Locati M, Camassi R, Rovida A, Ercolani E, Bernardini F, Castelli V, Caracciolo CH, Tertulliani A, Rossi A, Azzaro R, D'Amico S, Conte S, Rocchetti E (2016) DBMI15, the 2015 version of the Italian Macroseismic database. Istituto

Nazionale di Geofisica e Vulcanologia. doi:10.6092/INGV.IT-DBMI15

Lucente FP, Speranza F (2001) Belt bending driven by lateral bending of subducting lithospheric slab: geophysical evidences from the northern Apennines (Italy). Tectonophysics 337:53–64

Malinverno A, Ryan WBF (1986) Extension in Tyrrhenian sea and shortening inthe Apennines as result of arc migration driven by sinking of the lithosphere. Tectonics 5:227–254

Mantovani E, Viti M, Babbucci D, Cenni N, Tamburelli C, Vannucchi A, Falciani F, Fianchisti G, Baglione M, D'Intinosante V e Fabbroni P (2011) Sismotettonica dell'Appennino Settentrionale. Implicazioni per la pericolosità sismica della Toscana. Regione Toscana, Centro stampa Giunta Regione Toscana, Firenze, 88 pp

Mantovani E, Viti M, Babbucci D, Cenni N, Tamburelli C, Vannucchi A, Falciani F, Fianchisti G, Baglione M, D'Intinosante V, Fabbroni P, Martelli L, Baldi P e Bacchetti M (2013) Assetto tettonico e potenzialità sismogenetica dell'Appennino tosco-emiliano-romagnolo e Val Padana. Regione Emilia-Romagna-SGSS, Regione Toscana, Università di Siena-DSFTA, Centro stampa Regione Emilia-Romagna, 170 pp

Marroni M, Molli G, Ottria G, Pandolfi L (2001) Tectono-sedimentary evolutionof the external Liguride units (northern Apennines, Italy): insights in the pre-collisional history of a fossil ocean-continent transition zone. Geodin Acta 14:307–320

Marson I, Cernobori L, Nicolich R, Stoka M, Liotta D, Palmieri F, Velicogna I (1998) CROP 03 profile: a geophysical analysis of data and results. Mem Soc Geol Ital 52:123–137

Martelli L (2011) Quadro sismotettonico dell'Appennino emiliano-romagnolo e della Pianura Padana centrale. In: Atti del 30° convegno nazionale GNGTS, Trieste 14–17 novembre 2011, pp 152–156

Martelli L, Romani M (eds) (2013) Microzonazione sismica e analisi della condizione limite per l'emergenza delle aree epicentrali dei terremoti della pianura emiliana di maggio-giugno 2012 (Ordinanza del Commissario Delegato – Presidente della Regione Emilia-Romagna n 70/2012). Final report and Annexes in http://ambiente.regione.emilia-romagna.it/geologia/temi/sismica/speciale-terremoto/sisma-2012-ordinanza-70-13-11-2012-cartografia

Martelli L, Calabrese L, Ercolessi G, Severi P, Tarabusi G, Pileggi D, Rosselli S, Minarelli L, Pergalani F, Compagnoni M, Vannucchi G, Madiai C, Facciorusso J, Fioravante V, Giretti DD, Mucciarelli M, Priolo E, Laurenzano G (2013) Cartografia speditiva dell'amplificazione e del rischio di liquefazione nelle aree epicentrali del terremoto dell'Emilia 2012 (ML=5.9). Atti 32° convegno GNGTS, Trieste 19–21/11/2013, sessione 2.2, 262–267. Isbn: 978–88–902101-7-4

Martelli L, Sani F, Bonini M e Corti G (2014) Proposta preliminare per una nuova zonazione sismogenetica dell'Appennino settentrionale e aree limitrofe. In: Atti del 33° convegno nazionale GNGTS, Bologna 25–27 novembre 2014, sessione 2.1, questo volume

Martini IP, Sagri M (1993) Tectono-sedimentary characteristics of late Miocene-Quaternary extensional basins of the northern Apennines, Italy. Earth-Sci Rev 34:197–233

Meletti C, Valensise G (eds) (2004) Zonazione sismogenetica ZS9. In: Gruppo di Lavoro, Redazione della mappa di pericolosità sismica prevista dall'Ordinanza PCM 3274 del 20 marzo 2003, Rapporto conclusivo per il Dipartimento della Protezione Civile, INGV, Milano - Roma, App 2, 38 pp

Meletti C, Patacca E, Scandone P (2000) Construction of a seismotectonic model: the case of Italy. Pure Appl Geophys 157:11–35

Meletti C, Galadini F, Valensise G, Stucchi M, Basili R, Barba S, Vannucci G, Boschi E (2008) A seismic source zone model for the seismic hazard assessment of the Italian territory. Tectonophysics 450:85–108

NTC 2008 Norme Tecniche per le Costruzioni. Decreto 14/01/2008 del Ministero delle Infrastrutture. GU n 29 del 04/02/2008

OPCM 2006 Ordinanza del Presidente del Consiglio dei Ministri n 3519 del 28/04/2006 "Criteri generali per l'individuazione delle zone sismiche e per la formazione e l'aggiornamento degli elenchi delle medesime zone". GU n 108 del 11/05/2006

Ordaz M, Aguilar A, Arboleda J (2012) CRISIS2012, Ver 4.2 Program for computing seismic hazard, UNAM, México

Piccinini D, Chiarabba C, Augliera P, Monghidoro Earthquake Group (M.E.G.) (2006) Compression along the northern Apennines? Evidence from the mw 5.3 Monghidoro earthquake. Terra Nov. 18:89–94

Picotti V, Pazzaglia FJ (2008) A new active tectonic model for the construction of the northern Apennines mountain front near Bologna (Italy). J Geophys Res 113:B08412. doi:10.1029/2007JB005307

Pieri M, Groppi G (1981) Subsurface geological structure of the Po plain, Italy. Publication 414 Consiglio Nazionale Delle Ricerche. AGIP, Rome

Pondrelli S, Salinbeni S, Ekström G, Morelli A, Gasperini P, Vannucci G (2006) The Italian CMT dataset from 1977 to present. Phys Earth Planet Inter 159:286–303

Pondrelli S, Salimbeni S, Morelli A, Ekström G, Postpischl L, Vannucci G, Boschi E (2011) European-Mediterranean regional centroid moment tensor catalog: solutions for 2005-2008. Phys Earth Planet Int 185. doi:10.1016/j.pepi.2011.01.007

Pondrelli S, Salimbeni S, Perfetti P, Danecek P (2012) Quick regional centroid moment tensor solutions for the Emilia 2012 (northern Italy) seismic sequence. Ann Geophys 55(4):615–621. doi:10.4401/ag-6146

Rogledi S (2013) Structural setting of the central Po plain. Ingegneria Sismica, n 1-2, gennaio-giugno 2013, 126–139

Rossi M, Rogledi S, Barbacani G, Casadei D, Iaccarino S, Papani G (2002) Tectonostratigraphic architecture of Messinian piggyback basins of northern Apennines: the Emilia folds in the Reggio–Modena area and comparison with the Lombardia and Romagna sectors. Bollettino della Società Geologica Italiana 1:437–447

Rovida A, Camassi R, Gasperini P, Stucchi M (eds) (2011) CPTI11, the 2011 version of the Parametric catalogue of Italian earthquakes. INGV, Istituto Nazionale di Geofisica e Vulcanologia, Milano http://emidius.mi.ingv.it/CPTI

Rovida A, Locati M, Camassi R, Lolli B, Gasperini P (eds) (2016) CPTI15, the 2015 version of the Parametric catalogue of Italian earthquakes. Istituto Nazionale di Geofisica e Vulcanologia. doi:10.6092/INGV.IT-CPTI15

Sani F, Moratti G, Bonini M, Landi B, Tanini C, Piccardi L, Menichetti B (2001) A transect in southern Tuscany from

Baccinello basin to the Cetona ridge. Excursion 25–29 September 1997, Proceedings of the meeting 'The Elba Island:a key puzzle linking the Corso-Sardinian Massif and Adria'. Ofioliti 26 (2a) 381–400

Sani F, Bonini M, Piccardi L, Vannucci G, Delle Donne D, Benvenuti M, Moratti G, Corti G, Montanari D, Sedda L, Tanini C (2009) Late Pliocene-Quaternary evolution of outermost hinterland basins of the northern Apennines (Italy), and their relevance to active tectonics. In: Tondi E, Chiaraluce L, Roberts G (eds) Ten years after the Umbria-Marche earthquake, Central Italy, Tectonophysics, vol 476, pp 336–356. doi:10.1016/j.tecto.2008.12.012

Santulin M, Tamaro A, Rebez A, Martelli L, Sani F, Bovini M, Corti G, Sandron D, Slejko D (2014) Revision of seismic hazard in Emilia-Romagna based on a new seismic zonation of the northern Apennines. In proc. of 33° convegno nazionale GNGTS, Bologna 25–27 novembre 2014, sessione 2.1, pp 78–86

Scognamiglio L, Tinti E, Michelini A (2009) Real-time determination of seismic moment tensor for the Italian region. Bull Seism Soc Am 99:2223–2242 up-to-date catalogue at http://cnt.rm.ingv.it/tdmt

Selvaggi G, Amato A (1992) Subcrustal earthquakes in the northern Apennines (Italy): evidence for a still active subduction? Geophys Res Lett 19:2127–2130

Slejko D, Santulin M, Garcia J (2014) Seismic hazard estimates for the area of Pylos and surrounding region (SW Peloponnese) for seismic and tsunami risk assessment. Boll Geof Teor Appl 55:433–468. doi:10.4430/bgta0090

Stucchi M, Meletti C, Montaldo V, Crowley H, Calvi GM, Boschi E (2011) Seismic hazard assessment (2003–2009) for the Italian building code. Bull Seism Soc Am 101:1885–1911. doi:10.1785/0120100130

van der Meulen MJ, Kouwenhoven TJ, van der Zwaan GJ, Meulenkamp JE, Wortel MJR (1999) Late Miocene uplift in the Romagnan Apen-nines and the detachment of subducted lithosphere. Tectonophysics 315:319–335

Vannoli P, Basili R, Valensise G (2004) New geomorphic evidence for anticlinal growth driven by blind-thrust faulting along the northern Marche coastal belt (central Italy). J Seismol 8:297–312

Vannoli P, Burrato P, Valensise G (2014) The seismotectonics of the Po plain (northern Italy): tectonic diversity in a blind faulting domain. Pure Appl Geophys. doi:10.1007/s00024-014-0873-0

Weichert DH (1980) Estimation of the earthquake recurrence parameters for unequal observation periods for different magnitudes. Bull Seism Soc Am 70:1337–1346

Wortel MJR, Spakman W (1992) Structure and dynamics of subducted lithospherein the Mediterranean region. Proceedings Koninklijke Nederlandse AkademieWetenschappen 95:325–347